Chapter 2
Kinetic Boundary Condition at the Interface

Abstract The vapor–liquid interface can exist only where the bulk vapor phase and the bulk liquid phase of the same molecules coexist side by side. Therefore, all the properties of the interface are inevitably affected by the bulk liquid and vapor phases, and vice versa. The relation among these three constituents still remains unresolved in general nonequilibrium states. However, at least in a weak nonequilibrium state, the relations can be simplified and reformulated into a form of Kinetic Boundary Condition (KBC) at the vapor–liquid interface. In this chapter, from the microscopic point of view, we explain how the two bulk phases of vapor and liquid are connected via the KBC at the interface. The main tools used here are the nonequilibrium molecular dynamics simulation of vapor–liquid two-phase system and the Boltzmann equation for vapor. Our aims in this chapter are to establish the KBC at the interface by the molecular dynamics simulation and to reduce it into the boundary condition for the vapor flows in the fluid-dynamics region outside the Knudsen layer on the interface by the asymptotic analysis of the boundary-value problem of the Boltzmann equation for small Knudsen numbers.

2.1 Microscopic Description of Molecular Systems

The physical properties of materials consisted of a large number of molecules are resulted from some kinds of averages over a large number of molecules, because our utilization activities of materials are usually carried out in some scales considerably large compared with molecular scales. For example, the density of a fluid is always evaluated as an averaged mass of a number of molecules in a volume divided by the volume.

Consider the measurement of the temperature of a fluid by a thermometer. The motion of molecules forming the thermometer is in an equilibrium state as a result of the energy exchange with molecules in the fluid that contacts the thermometer. The total kinetic energy of molecules forming the thermometer is then translated into the temperature of thermometer, which is equal to the temperature of the fluid in the equilibrium state. In translating the kinetic energy to the temperature, we employ a fundamental relation in statistical mechanics [30]

S. Fujikawa et al., *Vapor-Liquid Interfaces, Bubbles and Droplets*, Heat and Mass Transfer, DOI 10.1007/978-3-642-18038-5_2, © Springer-Verlag Berlin Heidelberg 2011

$$\frac{3}{2}kT = \left\langle \frac{1}{2}m(\xi_x^2 + \xi_y^2 + \xi_z^2) \right\rangle, \tag{2.1}$$

where k is the Boltzmann constant, T is the temperature in the equilibrium state, m is the mass of a molecule, and (ξ_x, ξ_y, ξ_z) is the molecular velocity.[1] For the case of temperature measurement, the angle brackets $\langle \cdots \rangle$ in the right-hand side of Eq. (2.1) means the average over the molecules forming the thermometer and also a time average for some time duration of reading the scale of the thermometer. Thus, the macroscopic variables, e.g., T in the left-hand side of Eq. (2.1), are defined by some kinds of averages of microscopic variables, e.g., the molecular velocity (ξ_x, ξ_y, ξ_z) in the right-hand side of Eq. (2.1).

When the temperature and pressure of a material (liquids or gases) concerned are uniform over its some volume and the materials is at rest, the relations connecting the temperature, pressure, density, internal energy, and so on can be described without using the microscopic information. In the last century, such relations have been compiled and integrated into thermodynamics, which explains the relations among macroscopic variables of materials in equilibrium states and does not contain the microscopic information at least apparently. Although fluid dynamics can discuss behaviors of nonuniform and flowing liquids and gases, its foundation is supported by thermodynamics under the assumption of the local equilibrium, which requires that the fluid in a sufficiently small volume[2] is locally in an equilibrium state,[3] even if the temperature and pressure are not uniform and the fluid is flowing over large scales. The interface, however, is a thin layer by its definition, and thermodynamics (and fluid dynamics) in such a thin layer has not been established yet or may not be expected to be established. Therefore, we have to consider the vapor–liquid interface and its neighborhood from the microscopic point of view. For example, in Sect. 4.4, using molecular dynamics simulations, we demonstrate that when a spherical nanodroplet and the surrounding vapor are in an equilibrium state in the sense of statistical mechanics, the thermodynamical vapor–liquid equilibrium condition (an equality of chemical potentials of vapor and liquid) does not hold.

We start with a brief explanation of a general microscopic description of molecular systems.

---

[1] For simplicity, the fluid and the thermometer are assumed to be composed of monatomic molecules and at rest in the macroscopic sense. The formula $(m/2)\langle \xi_i^2 \rangle = kT/2$ $(i = x, y, z)$ is called the equipartition theorem or the law of equipartition of energy.

[2] The sufficiently small volume in fluid dynamics is sufficiently large in molecular scales so that it may contain a number of molecules. Thus, the macroscopic variables defined by some kinds of averages can be regarded as continuous functions of the space coordinates and the time. If the fluid is an ideal gas in the standard state, the number of molecules in a cube with a side-length 1 μm is 2.6867774×10^7. The number of molecules per unit volume is called the Loschmidt constant.

[3] The actualization of local equilibrium requires a sufficient number of molecular interactions (intermolecular collisions).

2.1.1 Equation of Motion

For simplicity, we deal with a single component system consisted of a large number of monatomic molecules, assuming that the motion of each molecule is determined by classical mechanics (without any quantum effects), the molecules are electrically neutral, and any types of association and dissociation do not occur. Then, Newton's equation of motion is the starting point:

$$m\frac{\mathrm{d}^2\boldsymbol{x}^{(i)}}{\mathrm{d}t^2} = \boldsymbol{f}^{(i)}, \quad (i = 1, 2, \ldots, N), \tag{2.2}$$

where m is the mass of a molecule, N is the total number of molecules in the system concerned, $\boldsymbol{x}^{(i)}$ is the position vector of the ith molecule, t is the time, and $\boldsymbol{f}^{(i)}$ is the force exerted on the ith molecule. Equation (2.2) can be written as

$$m\frac{\mathrm{d}^2x_j^{(i)}}{\mathrm{d}t^2} = f_j^{(i)}, \quad (i = 1, 2, \ldots, N;\ j = 1, 2, 3), \tag{2.3}$$

where $x_j^{(i)}$ and $f_j^{(i)}$ are the jth components of vectors $\boldsymbol{x}^{(i)}$ and $\boldsymbol{f}^{(i)}$, respectively. Once given an explicit form of the force $\boldsymbol{f}^{(i)}$ and initial positions and velocities of all molecules, Newton's equation of motion (2.2) can in principle be solved, e.g., numercally. All the macroscopic properties of materials can then be determined through their definitions in terms of some kinds of averages of the microscopic quantities, i.e., $\boldsymbol{x}^{(i)}$, $\mathrm{d}\boldsymbol{x}^{(i)}/\mathrm{d}t$, and $\mathrm{d}^2\boldsymbol{x}^{(i)}/\mathrm{d}t^2$ (or $\boldsymbol{f}^{(i)}$) for all molecules; the definitions of macroscopic variables, such as the temperature, density, velocity, pressure, internal energy, and so on, are shown in Sects. 2.1.3, 2.3.1, and 2.5.1.

In general, the force $\boldsymbol{f}^{(i)}$ includes external forces such as the gravity. The magnitude of acceleration due to gravity is, however, negligibly small compared with a typical intermolecular force in molecular scales in time and space, and hence we only consider $\boldsymbol{f}^{(i)}$ in Eq. (2.2) as the force acting between molecules, i.e., the intermolecular force.[4] Then, it seems to be plausible to assume that the force $\boldsymbol{f}^{(i)}$ is a conservative force, and its potential U is a function of intermolecular distances only. We further limit ourselves to the case that the potential U may be approximated as a pairwise and additive one, i.e.,

$$U = \frac{1}{2}\sum_{i=1}^{N}\sum_{\substack{k=1\\k\neq i}}^{N}\phi(r_{ik}), \tag{2.4}$$

where $r_{ik} = \left|\boldsymbol{x}^{(i)} - \boldsymbol{x}^{(k)}\right|$ is the distance between the ith molecule and the kth molecule ($i \neq k$) and ϕ is a function of intermolecular distance r_{ik}. The factor $1/2$

[4] Forces acting between atoms making up a molecule (covalent bonds, ionic bonds, and metallic bonds) are called the intramolecular forces.

in the right-hand side of Eq. (2.4) is introduced since the double sum with respect to i and k counts each pair twice. The force exerted on the ith molecule can then be defined by

$$\boldsymbol{f}^{(i)} = -\frac{\partial U}{\partial \boldsymbol{x}^{(i)}}, \tag{2.5}$$

and expressed in a component form as

$$f_j^{(i)} = -\sum_{\substack{k=1 \\ k\neq i}}^{N} \frac{\partial r_{ik}}{\partial x_j^{(i)}} \phi'(r_{ik}) = -\sum_{\substack{k=1 \\ k\neq i}}^{N} \frac{x_j^{(i)} - x_j^{(k)}}{r_{ik}} \phi'(r_{ik}), \tag{2.6}$$

or in a vector form as

$$\boldsymbol{f}^{(i)} = -\sum_{\substack{k=1 \\ k\neq i}}^{N} \frac{\boldsymbol{x}^{(i)} - \boldsymbol{x}^{(k)}}{r_{ik}} \phi'(r_{ik}), \tag{2.7}$$

where $\phi'(r_{ik})$ denotes the derivative of ϕ with respect to r_{ik}. The pairwise and additive potentials are widely used in molecular dynamics (MD) simulations of liquids and gases [1, 11], although the complete validation has not been given. On the other hand, multi-body potentials are used for various MD simulations of crystalline materials such as graphite, diamond, and carbon nanotube [6].

Introducing the generalized momenta $p_j^{(i)}$ conjugate to the generalized coordinates $q_j^{(i)}$, Newton's equation of motion (2.3) with Eq. (2.6) can be reformulated to the equations of motion in Hamilton's form, or Hamilton's canonical equations of motion [22]:

$$\frac{\mathrm{d}q_j^{(i)}}{\mathrm{d}t} = \frac{\partial \mathcal{H}}{\partial p_j^{(i)}}, \quad \frac{\mathrm{d}p_j^{(i)}}{\mathrm{d}t} = -\frac{\partial \mathcal{H}}{\partial q_j^{(i)}}, \quad (i = 1, 2, \ldots, N;\ j = 1, 2, 3). \tag{2.8}$$

Here,

$$p_j^{(i)} = m\frac{\mathrm{d}x_j^{(i)}}{\mathrm{d}t}, \quad q_j^{(i)} = x_j^{(i)}, \tag{2.9}$$

$$\mathcal{H} = \sum_{n=1}^{N} \left[\frac{1}{2} \sum_{k=1}^{3} \frac{p_k^{(n)} p_k^{(n)}}{m} + \frac{1}{2} \sum_{\substack{k=1 \\ k\neq n}}^{N} \phi(r_{nk}) \right], \tag{2.10}$$

where $\mathcal{H}$ is the Hamiltonian of the whole system. Note that we confine ourselves to the molecular system of N monatomic molecules, and hence the kinetic energy included in the Hamiltonian $\mathcal{H}$ is that of translational motions only [the inclusion of

the internal rotational motions of a polyatomic molecule into Eqs. (2.8), (2.9), and (2.10) is straightforward]. Since the Hamiltonian $\mathcal{H}$ defined by Eq. (2.10) does not depend explicitly on the time t, it is a global constant of the motion and we write $\mathcal{H} = \mathcal{E}$, where $\mathcal{E}$ is the total energy of the system.

2.1.2 Liouville Equation

An arbitrary state of the N molecular system can be specified by using the $6N$-dimensional phase space $(\boldsymbol{q}, \boldsymbol{p})$, where $\boldsymbol{q} = (q_1^{(1)}, q_2^{(1)}, q_3^{(1)}, q_1^{(2)}, \ldots, q_2^{(N)}, q_3^{(N)})$ and $\boldsymbol{p} = (p_1^{(1)}, p_2^{(1)}, p_3^{(1)}, p_1^{(2)}, \ldots, p_2^{(N)}, p_3^{(N)})$ [22, 30, 32]. The results derived from the concept of the phase space should be the same as those obtained from the solutions of Newton's equation of motion (2.3) with Eq. (2.6), while the former is much more suitable for the deduction of macroscopic properties from the microscopic information, because the macroscopic properties are associated with some kinds of averages over a number of molecules. The $6N$-dimensional phase space is sometimes called the Γ-space.

Specifying an arbitrary point $(\boldsymbol{q}, \boldsymbol{p})$ in the $6N$-dimensional phase space at a given time t is equivalent to specifying a set of initial conditions of Newton's equations of motion for N molecules. From the existence and uniqueness of the solution of initial-value problem of a set of Newton's equations of motion (a set of ordinary differential equations), there exists a trajectory of solution that passes through the specified arbitrary point $(\boldsymbol{q}, \boldsymbol{p})$ in the phase space at the time. That is, the phase space is filled with the trajectories of solutions of a set of Newton's equations of motion and a point in the phase space represents a state of the N molecular system.

The density distribution function (probability density function) $F(\boldsymbol{q}, \boldsymbol{p}, t)$ in the phase space is now defined by

$$\mathrm{d}P = F(\boldsymbol{q}, \boldsymbol{p}, t)\, \mathrm{d}\boldsymbol{q}\, \mathrm{d}\boldsymbol{p}, \tag{2.11}$$

where $\mathrm{d}P$ is the probability that a point $(\boldsymbol{q}, \boldsymbol{p})$, moving in the phase space according to Newton's equation of motion, lies in a $6N$-dimensional volume element $\mathrm{d}\boldsymbol{q}\, \mathrm{d}\boldsymbol{p} = \mathrm{d}q_1^{(1)} \mathrm{d}q_2^{(1)} \cdots \mathrm{d}q_3^{(N)} \mathrm{d}p_1^{(1)} \mathrm{d}p_2^{(1)} \cdots \mathrm{d}p_3^{(N)}$ at a time t. Thus, the probability of finding the system of N molecules in a region χ in the phase space is

$$P(\chi) = \int_{\chi} F(\boldsymbol{q}, \boldsymbol{p}, t)\, \mathrm{d}\boldsymbol{q}\, \mathrm{d}\boldsymbol{p}, \tag{2.12}$$

where the integration is taken over the region χ. If χ is the whole $6N$-dimensional space, then $P(\chi) = 1$. The expected value of an arbitrary function $G(\boldsymbol{q}, \boldsymbol{p})$ is given by

$$\int G(\boldsymbol{q}, \boldsymbol{p}) F(\boldsymbol{q}, \boldsymbol{p}, t)\, \mathrm{d}\boldsymbol{q}\, \mathrm{d}\boldsymbol{p}. \tag{2.13}$$

From the conservation of probability, in the same manner as the derivation of equation of mass continuity in fluid dynamics, we have [22, 30, 32]

$$\frac{\mathrm{d}F}{\mathrm{d}t} = \frac{\partial F}{\partial t} + \sum_{i=1}^{N}\sum_{j=1}^{3}\left[\frac{\partial}{\partial q_j^{(i)}}\left(F\frac{\mathrm{d}q_j^{(i)}}{\mathrm{d}t}\right) + \frac{\partial}{\partial p_j^{(i)}}\left(F\frac{\mathrm{d}p_j^{(i)}}{\mathrm{d}t}\right)\right] = 0, \tag{2.14}$$

where $\mathrm{d}F/\mathrm{d}t$ is the total time derivative of F. Expanding the derivatives with respect to $q_j^{(i)}$ and $p_j^{(i)}$ in Eq. (2.14) and applying the equations of motion in Hamilton's form (2.8), we can transform Eq. (2.14) into

$$\frac{\partial F}{\partial t} + \sum_{i=1}^{N}\sum_{j=1}^{3}\left(\frac{\mathrm{d}q_j^{(i)}}{\mathrm{d}t}\frac{\partial F}{\partial q_j^{(i)}} + \frac{\mathrm{d}p_j^{(i)}}{\mathrm{d}t}\frac{\partial F}{\partial p_j^{(i)}}\right) = 0. \tag{2.15}$$

Equation (2.15) is called the Liouville equation. Using Eq. (2.9) and Newton's equation of motion (2.3) in Eq. (2.15), we have

$$\frac{\partial F}{\partial t} + \sum_{i=1}^{N}\sum_{j=1}^{3}\left(\frac{p_j^{(i)}}{m}\frac{\partial F}{\partial q_j^{(i)}} + f_j^{(i)}\frac{\partial F}{\partial p_j^{(i)}}\right) = 0. \tag{2.16}$$

Equation (2.16) is also called the Liouville equation.

If an isolated system is in an equilibrium state, then the probability density F must be time independent and we have

$$\sum_{i=1}^{N}\sum_{j=1}^{3}\left(\frac{p_j^{(i)}}{m}\frac{\partial F}{\partial q_j^{(i)}} + f_j^{(i)}\frac{\partial F}{\partial p_j^{(i)}}\right) = 0. \tag{2.17}$$

This means that the flow in the phase space is steady and incompressible in the sense of fluid dynamics [22, 30, 32]. In general nonequilibrium states, Eq. (2.17) does not hold and we have to return to the Liouville equation (2.16).

2.1.3 Definitions of Macroscopic Variables and Equations in Fluid Dynamics

The formal relations between microscopic and macroscopic variables can readily be derived from the Liouville equation (2.16) by the method of Irving and Kirkwood [15]. The method is superior in that the definitions of macroscopic variables can be applied to those in nonequilibrium states for both liquids and gases, and the resulting definitions are suitable for the use in the analysis of the data obtained by MD simulations. Note that if we restrict ourselves to the case that the fluid is an ideal gas, the definitions of macroscopic variables have been established in the kinetic

theory of gases (molecular gas dynamics) in terms not of the probability density F but of the velocity distribution function of gas molecules [35]. The kinetic theory of gases are summarized in Sect. 2.3.

In the following, we derive the equations in fluid dynamics (conservation equations of mass, momentum, and energy) from the Liouville equation (2.16) by the method of Irving and Kirkwood [15] with a small modification for the later use in Sect. 2.2. In the original paper [15], the Dirac delta function is used instead of a scalar function χ defined below.

To begin with, we define an averaged fluid density as

$$\rho(\boldsymbol{x}, t) = \frac{m}{h^3} \sum_{i=1}^{N} \int \chi(\boldsymbol{q}^{(i)}, \boldsymbol{x}; h) F(\boldsymbol{q}, \boldsymbol{p}, t) \, \mathrm{d}\boldsymbol{q} \, \mathrm{d}\boldsymbol{p}, \tag{2.18}$$

where the integration is taken over the whole $6N$-dimensional phase space and

$$\chi(\boldsymbol{q}^{(i)}, \boldsymbol{x}; h) = \begin{cases} 1 & \left| q_j^{(i)} - x_j \right| \leqq h/2 \text{ for } j = 1, 2, 3, \\ 0 & \text{otherwise.} \end{cases} \tag{2.19}$$

That is, if the ith molecule is in a cube with a side-length h centered at $\boldsymbol{x}$, then $\chi = 1$ and the integration yields the expected value that one will find the ith molecule in the cube (Fig. 2.1). Therefore, the right-hand side of Eq. (2.18) is the expected value of the number of molecules in the cube multiplied by m/h^3, which is the averaged fluid density ρ. Note that the introduction of the function χ is a coarse-graining process. Although the side-length h of the cube is arbitrary, it should be small compared with some length scale that is to be resolved.

Similarly, an averaged fluid momentum per unit volume and an averaged total energy of fluid per unit volume are defined as

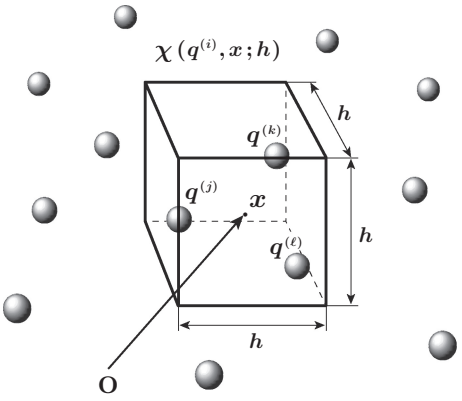

Fig. 2.1 The value of the scalar function $\chi(\boldsymbol{q}^{(i)}, \boldsymbol{x}; h)$ is equal to unity if the ith molecule is contained in a cube with a side-length h centered at $\boldsymbol{x}$

$$\rho(\boldsymbol{x},t)v_j(\boldsymbol{x},t)=\frac{1}{h^3}\sum_{i=1}^{N}\int\chi(\boldsymbol{q}^{(i)},\boldsymbol{x},h)p_j^{(i)}F(\boldsymbol{q},\boldsymbol{p},t)\,\mathrm{d}\boldsymbol{q}\,\mathrm{d}\boldsymbol{p},\tag{2.20}$$

$$\rho(\boldsymbol{x},t)E(\boldsymbol{x},t)=\frac{1}{h^3}\sum_{i=1}^{N}\int\chi(\boldsymbol{q}^{(i)},\boldsymbol{x},h)e^{(i)}F(\boldsymbol{q},\boldsymbol{p},t)\,\mathrm{d}\boldsymbol{q}\,\mathrm{d}\boldsymbol{p},\tag{2.21}$$

$$e^{(i)}=\frac{1}{2}\sum_{j=1}^{3}\frac{p_j^{(i)}p_j^{(i)}}{m}+\frac{1}{2}\sum_{\substack{k=1\\k\neq i}}^{N}\phi(r_{ik}),\tag{2.22}$$

where Eq. (2.10) is used for the definition of $e^{(i)}$, the sum of the kinetic and potential energies of the ith molecule.[5] Thus, the fluid velocity v_j and the total energy of fluid per unit mass E are defined.[6]

The conservation law of mass of a fluid is expressed in a partial differential equation, which can be derived from the Liouville equation (2.16) in the following manner. Multiplying Eq. (2.16) by $\chi^{(n)}=\chi(\boldsymbol{q}^{(n)},\boldsymbol{x},h)$, we have

$$\frac{\partial}{\partial t}(\chi^{(n)}F)+\sum_{i=1}^{N}\sum_{j=1}^{3}\left(\chi^{(n)}\frac{p_j^{(i)}}{m}\frac{\partial F}{\partial q_j^{(i)}}+\chi^{(n)}f_j^{(i)}\frac{\partial F}{\partial p_j^{(i)}}\right)=0.\tag{2.23}$$

Integrating Eq. (2.23) over the whole phase space gives

$$\begin{aligned}\frac{\partial}{\partial t}\int\chi^{(n)}F\,\mathrm{d}\boldsymbol{q}\,\mathrm{d}\boldsymbol{p}+\sum_{i=1}^{N}\sum_{j=1}^{3}\Bigg(&\int\chi^{(n)}\frac{p_j^{(i)}}{m}\frac{\partial F}{\partial q_j^{(i)}}\,\mathrm{d}\boldsymbol{q}\,\mathrm{d}\boldsymbol{p}\\&+\int\chi^{(n)}f_j^{(i)}\frac{\partial F}{\partial p_j^{(i)}}\,\mathrm{d}\boldsymbol{q}\,\mathrm{d}\boldsymbol{p}\Bigg)=0.\end{aligned}\tag{2.24}$$

With the aid of the Gauss divergence theorem, the following equations hold for an arbitrary function G,

$$\sum_{i=1}^{N}\sum_{j=1}^{3}\int_{\Omega_q}G(\boldsymbol{q})\frac{\partial F}{\partial q_j^{(i)}}\,\mathrm{d}\boldsymbol{q}=-\sum_{i=1}^{N}\sum_{j=1}^{3}\int_{\Omega_q}\frac{\partial G}{\partial q_j^{(i)}}F\,\mathrm{d}\boldsymbol{q},\tag{2.25}$$

$$\sum_{i=1}^{N}\sum_{j=1}^{3}\int_{\Omega_p}G(\boldsymbol{p})\frac{\partial F}{\partial p_j^{(i)}}\,\mathrm{d}\boldsymbol{p}=-\sum_{i=1}^{N}\sum_{j=1}^{3}\int_{\Omega_p}\frac{\partial G}{\partial p_j^{(i)}}F\,\mathrm{d}\boldsymbol{p},\tag{2.26}$$

[5] The potential energy of the ith molecule is defined only formally. It is the total potential energy of all molecules that has the physical meaning.

[6] In Chap. 5 and in Appendix B, the internal energy per unit mass of fluid is denoted by e.

if the probability density F falls off rapidly outside a bounded region Ω_q in the $3N$-dimensional space of $\boldsymbol{q}$ in the case of Eq. (2.25) and outside a bounded region Ω_p in the $3N$-dimensional space of $\boldsymbol{p}$ in the case of Eq. (2.26).

Using Eqs. (2.25) and (2.26), we can rewrite Eq. (2.24) into

$$\frac{\partial}{\partial t}\int \chi^{(n)} F \,\mathrm{d}\boldsymbol{q}\,\mathrm{d}\boldsymbol{p} - \sum_{i=1}^{N}\sum_{j=1}^{3}\left[\int \frac{\partial}{\partial q_j^{(i)}}\left(\chi^{(n)}\frac{p_j^{(i)}}{m}\right) F \,\mathrm{d}\boldsymbol{q}\,\mathrm{d}\boldsymbol{p} + \int \frac{\partial}{\partial p_j^{(i)}}\left(\chi^{(n)} f_j^{(i)}\right) F \,\mathrm{d}\boldsymbol{q}\,\mathrm{d}\boldsymbol{p}\right] = 0. \quad (2.27)$$

Since $\chi^{(n)}$ and $f_j^{(i)}$ are independent of $p_j^{(i)}$, the differentiation of $\chi^{(n)} f_j^{(i)}$ with respect to $p_j^{(i)}$ vanishes, i.e.,

$$\frac{\partial}{\partial p_j^{(i)}}\left(\chi^{(n)} f_j^{(i)}\right) = 0. \quad (2.28)$$

From the definition of the function χ, Eq. (2.19), we have

$$\sum_{i=1}^{N}\frac{\partial}{\partial q_j^{(i)}}\left(\chi^{(n)}\frac{p_j^{(i)}}{m}\right) = \frac{\partial}{\partial q_j^{(n)}}\left(\chi^{(n)}\frac{p_j^{(n)}}{m}\right) = -\frac{\partial}{\partial x_j}\left(\chi^{(n)}\frac{p_j^{(n)}}{m}\right), \quad (2.29)$$

where in the last equality we used

$$\frac{\partial \chi^{(n)}}{\partial q_j^{(n)}} = -\frac{\partial \chi^{(n)}}{\partial x_j}. \quad (2.30)$$

Substituting Eqs. (2.28) and (2.29) into Eq. (2.27) and taking the sum over all n, we obtain the equation of mass continuity in fluid dynamics,

$$\frac{\partial \rho}{\partial t} + \sum_{j=1}^{3}\frac{\partial \rho v_j}{\partial x_j} = 0, \quad (2.31)$$

where the definitions of ρ and ρv_j, Eqs. (2.18) and (2.20), are used. Equation (2.31) with the definitions of ρ and v_j does not require the assumption of local equilibrium unlike in the case of fluid dynamics.[7]

[7] The only requirement is that ρ and v_j are continuously differentiable functions of $\boldsymbol{x}$ and t. This will be satisfied by choosing h in the function χ so that the cube with a side-length h centered at $\boldsymbol{x}$ contains a large number of molecules. If the fluid is a gas, this does not warrant the local equilibrium, because the mean free path of gas molecules can be very large compared with h.

In the same manner as the derivation of Eq. (2.27), we can derive the equations of momentum conservation of nth molecule

$$\frac{\partial}{\partial t}\int \chi^{(n)} p_k^{(n)} F \,\mathrm{d}\boldsymbol{q}\,\mathrm{d}\boldsymbol{p} - \sum_{i=1}^{N}\sum_{j=1}^{3}\left[\int \frac{\partial}{\partial q_j^{(i)}}\left(\chi^{(n)}\frac{p_k^{(n)} p_j^{(i)}}{m}\right) F \,\mathrm{d}\boldsymbol{q}\,\mathrm{d}\boldsymbol{p} + \int \frac{\partial}{\partial p_j^{(i)}}\left(\chi^{(n)} p_k^{(n)} f_j^{(i)}\right) F \,\mathrm{d}\boldsymbol{q}\,\mathrm{d}\boldsymbol{p}\right] = 0, \quad (k = 1, 2, 3), \tag{2.32}$$

where Eq. (2.20) is used. By making use of Eqs. (2.28) and (2.30), Eq. (2.32) can be rewritten into

$$\frac{\partial}{\partial t}\int \chi^{(n)} p_k^{(n)} F \,\mathrm{d}\boldsymbol{q}\,\mathrm{d}\boldsymbol{p} + \sum_{j=1}^{3}\frac{\partial}{\partial x_j}\int \chi^{(n)}\frac{p_k^{(n)} p_j^{(n)}}{m} F \,\mathrm{d}\boldsymbol{q}\,\mathrm{d}\boldsymbol{p} - \int \chi^{(n)} f_k^{(n)} F \,\mathrm{d}\boldsymbol{q}\,\mathrm{d}\boldsymbol{p} = 0, \quad (k = 1, 2, 3). \tag{2.33}$$

The third term in Eq. (2.33) can be transformed to yield[8]

$$\frac{\partial}{\partial t}\int \chi^{(n)} p_k^{(n)} F \,\mathrm{d}\boldsymbol{q}\,\mathrm{d}\boldsymbol{p} + \sum_{j=1}^{3}\frac{\partial}{\partial x_j}\int \chi^{(n)}\frac{p_k^{(n)} p_j^{(n)}}{m} F \,\mathrm{d}\boldsymbol{q}\,\mathrm{d}\boldsymbol{p} - \sum_{j=1}^{3}\frac{\partial}{\partial x_j}\int \frac{1}{3}\left(x_j - q_j^{(n)} + \frac{h}{2}\right)\chi^{(n)} f_k^{(n)} F \,\mathrm{d}\boldsymbol{q}\,\mathrm{d}\boldsymbol{p} = 0, \quad (k = 1, 2, 3). \tag{2.34}$$

Taking the sum over n, we should have the conservation equation of the momentum of the fluid per unit volume,

$$\frac{\partial \rho v_k}{\partial t} + \sum_{j=1}^{3}\frac{\partial}{\partial x_j}\left(\rho v_k v_j + P_{kj}\right) = 0, \quad (k = 1, 2, 3), \tag{2.35}$$

where the microscopic definition of the stress tensor P_{kj} is given as

---

In the case that the fluid is a liquid, this may be a sufficient condition for the local equilibrium, because the mean free path of liquid molecules is usually comparable with or less than a typical diameter of a molecule.

[8] The factor $\frac{1}{3}$ in Eq. (2.34) is an ideal limit of $N \to \infty$ in equilibrium states. The stress tensor in the original paper [15] is different from this and much more cumbersome.

$$P_{kj} = \frac{1}{h^3}\sum_{n=1}^{N}\int\left[\frac{p_k^{(n)}p_j^{(n)}}{m} - \frac{1}{3}\left(x_j - q_j^{(n)} + \frac{h}{2}\right) f_k^{(n)}\right]\chi^{(n)}F\,\mathrm{d}\boldsymbol{q}\,\mathrm{d}\boldsymbol{p}$$

$$-\rho v_j v_k, \quad (j,k=1,2,3). \tag{2.36}$$

If the fluid is in a uniform equilibrium state at rest, then $v_j = 0$ and $P_{kj} = P\delta_{kj}$, where δ_{kj} is the Kronecker delta and pressure P is given by

$$P = \frac{1}{3h^3}\sum_{n=1}^{N}\sum_{k=1}^{3}\int\left[\frac{p_k^{(n)}p_k^{(n)}}{m} - \left(x_k - q_k^{(n)} + \frac{h}{2}\right) f_k^{(n)}\right]\chi^{(n)}F\,\mathrm{d}\boldsymbol{q}\,\mathrm{d}\boldsymbol{p}. \tag{2.37}$$

The energy conservation equation for the nth molecule, the counterpart of Eq. (2.34), is

$$\frac{\partial}{\partial t}\int\chi^{(n)}e^{(n)}F\,\mathrm{d}\boldsymbol{q}\,\mathrm{d}\boldsymbol{p} + \sum_{j=1}^{3}\frac{\partial}{\partial x_j}\int\chi^{(n)}e^{(n)}\frac{p_j^{(n)}}{m}F\,\mathrm{d}\boldsymbol{q}\,\mathrm{d}\boldsymbol{p}$$

$$-\sum_{j=1}^{3}\frac{\partial}{\partial x_j}\int\left(x_j - q_j^{(n)} + \frac{h}{2}\right)\chi^{(n)}\frac{p_j^{(n)}}{m}f_j^{(n)}F\,\mathrm{d}\boldsymbol{q}\,\mathrm{d}\boldsymbol{p} = 0. \tag{2.38}$$

After taking the sum over n, the conservation equation of the total energy of the fluid per unit volume and the microscopic definition of the heat flux Q_j are obtained as

$$\frac{\partial\rho E}{\partial t} + \sum_{j=1}^{3}\frac{\partial}{\partial x_j}\left(\rho E v_j + \sum_{i=1}^{3}P_{ij}v_i + Q_j\right) = 0, \tag{2.39}$$

$$Q_j = \frac{1}{h^3}\sum_{n=1}^{N}\int\left[e^{(n)} - \left(x_j - q_j^{(n)} + \frac{h}{2}\right)f_j^{(n)}\right]\frac{p_j^{(n)}}{m}\chi^{(n)}F\,\mathrm{d}\boldsymbol{q}\,\mathrm{d}\boldsymbol{p}$$

$$-\left(\rho E v_j + \sum_{i=1}^{3}P_{ij}v_i\right), \quad (j=1,2,3). \tag{2.40}$$

It may be instructive to compare the above results with the definitions of macroscopic variables in the kinetic theory of gases [35]. The definitions of the stress tensor and the heat flux in the kinetic theory of gases are given as follows:

$$P_{ij} = \int(\xi_i - v_i)(\xi_j - v_j)f(\boldsymbol{x},\boldsymbol{\xi},t)\,\mathrm{d}\boldsymbol{\xi}$$

$$= \int\xi_i\xi_j f(\boldsymbol{x},\boldsymbol{\xi},t)\,\mathrm{d}\boldsymbol{\xi} - \rho v_i v_j, \quad (i,j,=1,2,3), \tag{2.41}$$

$$Q_j = \int \frac{1}{2}(\xi_j - v_j) \sum_{i=1}^{3} (\xi_i - v_i)^2 f(\boldsymbol{x}, \boldsymbol{\xi}, t)\, \mathrm{d}\boldsymbol{\xi}$$
$$= \int \xi_j \frac{1}{2} \sum_{i=1}^{3} \xi_i^2 f(\boldsymbol{x}, \boldsymbol{\xi}, t)\, \mathrm{d}\boldsymbol{\xi} - \left[\rho \left(\frac{3}{2} RT + \frac{1}{2} \sum_{i=1}^{3} v_i^2 \right) v_j + \sum_{i=1}^{3} p_{ij} v_i \right], \quad (j = 1, 2, 3), \quad (2.42)$$

where ξ_i is the ith component of molecular velocity, T is the temperature, $R = k/m$ is the gas constant (per unit mass), the integration is taken over the 3-dimensional space of molecular velocity $\boldsymbol{\xi}$, and $f(\boldsymbol{x}, \boldsymbol{\xi}, t)$ is the velocity distribution function of gas molecules, which gives the gas density

$$\rho = \int f(\boldsymbol{x}, \boldsymbol{\xi}, t)\, \mathrm{d}\boldsymbol{\xi}. \quad (2.43)$$

The precise definition of the velocity distribution function $f(\boldsymbol{x}, \boldsymbol{\xi}, t)$ is given in Sect. 2.3.1. Equations (2.41) and (2.42) are also applicable to general nonequilibrium states with the definition of temperature

$$\frac{3}{2} \rho RT = \int \frac{1}{2} \sum_{i=1}^{3} \xi_i^2 f\, \mathrm{d}\boldsymbol{\xi} - \frac{1}{2} \rho \sum_{i=1}^{3} v_i^2. \quad (2.44)$$

As compared with Eqs. (2.36) and (2.40), one can see that the contribution of intermolecular force is neglected in Eqs. (2.41) and (2.42).

Thus, the microscopic definitions of the stress tensor and the heat flux are extended to nonequilibrium states in fluids including liquids where the intermolecular force cannot be neglected. They are used for the analysis of results from MD simulations. For the definition of temperature,

$$\frac{3}{2} kT = \sum_{i=1}^{N} \int \chi(\boldsymbol{q}^{(i)} - \boldsymbol{x}; h) \frac{1}{2} \sum_{j=1}^{3} \frac{p_j^{(i)} p_j^{(i)}}{m} F(\boldsymbol{q}, \boldsymbol{p}, t)\, \mathrm{d}\boldsymbol{q}\, \mathrm{d}\boldsymbol{p} - \frac{m}{2} \sum_{i=1}^{3} v_i^2, \quad (2.45)$$

is used in MD simulations, instead of Eq. (2.44).

We have derived the equations for conservation laws of macroscopic variables, Eqs. (2.31), (2.35), and (2.39), with the definitions of macroscopic variables, Eqs. (2.18), (2.20), (2.21), (2.36), (2.40), and (2.45). They can be applied to general nonequilibrium states of liquids and gases, for which we cannot expect (i) the thermodynamic relations (or the assumption of local equilibrium), (ii) the stress tensor of the Newtonian fluid, and (iii) the heat flux based on the Fourier law. For example, it is well known that the stress tensor for a slightly rarefied gas contains terms related to temperature gradient, called the thermal stress [35], which does not appear in equations of fluid dynamics (see Appendix B at the end of this book).

Since our target is the vapor–liquid interface, we have to know the behavior of molecules in the liquid phase. For this purpose, we use the MD simulations for the vapor–liquid two phase system.

2.2 Molecular Dynamics Simulation

In the preceding subsection, we have given the definitions of macroscopic variables in terms of the microscopic information. They can be applied to liquids and gases in general nonequilibrium states, and expressed in appropriate forms for the analysis in MD simulation. Now, we move on to the explanation of the method of MD simulations.

The standard method of MD simulation numerically solves Newton's equation of motion (2.3) for a number of molecules confined in a simulation box fixed in a physical coordinate system. The total number of molecules in the box is unchanged during the simulation if an appropriate boundary condition on the surface of the box is imposed. Such a method of simulation is called NVE simulation because the number of molecules, N, the volume of the system, V, and the total energy of molecules, E, are constant in the simulation except for numerical errors (mainly truncation errors) in the total energy. It is possible and sometimes preferred to perform simulations with a constant temperature (NVT simulation) or those with constant temperature and pressure (NPT simulation) [1, 13]. However, NVT simulation and NPT simulation solve some dynamical systems different from Newton's equation of motion (2.3) and the Liouville equation (2.16). The differences resulted from the differences from Newton's equation of motion have not been figured out in nonequilibrium MD simulations.[9] In this book, we concentrate on the dynamics of molecules based on Newton's equation of motion (2.3), although not restricted to NVE simulations.

2.2.1 Lennard-Jones Potential and Normalization of Variables

In MD simulations, the most widely used pairwise additive potential is the Lennard-Jones 12-6 potential [23],

$$U = \frac{1}{2}\sum_{i=1}^{N}\sum_{\substack{k=1\\k\neq i}}^{N}\phi(r_{ik}), \quad \phi(r_{ik}) = 4\epsilon\left[\left(\frac{\sigma}{r_{ik}}\right)^{12} - \left(\frac{\sigma}{r_{ik}}\right)^{6}\right], \tag{2.46}$$

where ϵ (J) and σ (m) are the energy and length parameters of Lennard-Jones 12-6 potential. Using these two parameters and the molecular mass m, Newton's equation of motion (2.3) can be nondimensionalized as

[9] The macroscopic properties in equilibrium states should not be different by the difference of simulation methods.

$$\frac{\mathrm{d}^2\hat{x}_j^{(i)}}{\mathrm{d}\hat{t}^2} = \hat{f}_j^{(i)}, \tag{2.47}$$

where

$$\hat{x}_j^{(i)} = \frac{x_j^{(i)}}{\sigma}, \quad \hat{t} = \frac{t}{\sigma\sqrt{m/\epsilon}}, \quad \hat{f}_j^{(i)} = \frac{f_j^{(i)}}{\epsilon/\sigma}. \tag{2.48}$$

The nondimensional quantities are signified by $\hat{}$. Then, from Eq. (2.6), the nondimensionalized intermolecular force $\hat{f}_j^{(i)}$ is given by

$$\hat{f}_j^{(i)} = -\sum_{\substack{k=1 \\ k\neq i}}^{N} \frac{\hat{x}_j^{(i)} - \hat{x}_j^{(k)}}{\hat{r}_{ik}} \hat{\phi}'(\hat{r}_{ik}), \tag{2.49}$$

where

$$\hat{\phi}(\hat{r}_{ik}) = 4\left[\left(\frac{1}{\hat{r}_{ik}}\right)^{12} - \left(\frac{1}{\hat{r}_{ik}}\right)^{6}\right], \quad \hat{r}_{ik} = \left|\hat{\boldsymbol{x}}^{(i)} - \hat{\boldsymbol{x}}^{(k)}\right|. \tag{2.50}$$

The macroscopic variables are also nondimensionalized as follows:

$$\hat{\rho} = \frac{\sigma^3\rho}{m}, \quad \hat{T} = \frac{kT}{\epsilon}, \quad \hat{v}_j = \frac{v_j}{\sqrt{\epsilon/m}}, \quad \hat{P}_{ij} = \frac{\sigma^3 P_{ij}}{\epsilon}, \quad \hat{Q}_j = \frac{\sigma^3 m^{1/2} Q_j}{\epsilon^{3/2}}. \tag{2.51}$$

In Fig. 2.2, the nondimensionalized Lennard-Jones 12-6 potential $\hat{\phi}(\hat{r})$ and its derivative with respect to the argument, $\hat{\phi}'(\hat{r})$, are shown in a solid curve and dashed curve, respectively. The potential $\hat{\phi}(\hat{r})$ has a minimum at $\hat{r} = 2^{1/6}$, at which a strong repulsive force ($\hat{r} < 2^{1/6}$) is switched to an attractive force ($\hat{r} > 2^{1/6}$). The repulsive force behaves like $\hat{r}^{-13}$ and the asymptotic form of the tail of attractive force is $\hat{r}^{-7}$ as $\hat{r} \to \infty$.

Figure 2.2 suggests that $\hat{r} = 1$ ($r = \sigma$) is a reasonable measure of the diameter of the molecule modeled by the Lennard-Jones 12-6 potential. The depth of potential well, i.e., the minimum of $\hat{\phi}$, corresponds to $\phi = \epsilon$ and indicates the strength of molecular interaction. Thanks to a number of simulation studies up to now, the Lennard-Jones parameters ϵ and σ suitable for modeling simple molecules such as Ar, Ne, Kr, N, O have been tabulated; for example, $(\epsilon/k, \sigma) =$ (119.8 K, 0.341 nm) for Ar, (47.0 K, 0.272 nm) for Ne, (164.0 K, 0.383 nm) for Kr, (37.3 K, 0.331 nm) for N, (61.6 K, 0.295 nm) for O [1], where the Boltzmann constant $k = 1.3806504 \times 10^{-23}$ J/K.

Before proceeding to subsections for numerical method, we note that the nondimensionalization of variables in Eqs. (2.48), (2.49), (2.50), and (2.51) are defined by the quantities in molecular scales. Effects of much larger scales in space and

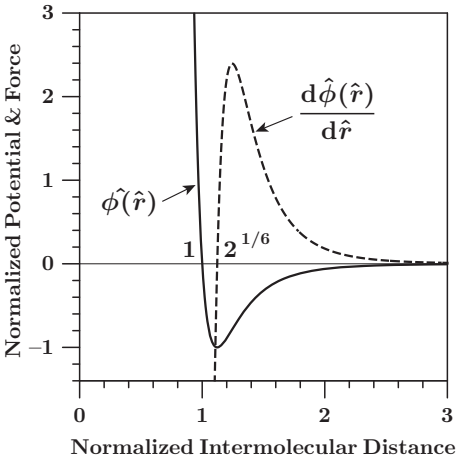

Fig. 2.2 The nondimensionalized Lennard-Jones 12-6 potential $\hat{\phi}(\hat{r})$ (*solid curve*) and its derivative with respect to the argument $\hat{\phi}'(\hat{r})$ (*dashed curve*)

time may therefore slip through standard numerical methods usually used in MD simulations.[10] We focus on molecular phenomena in molecular scales.

2.2.2 Finite Difference Method

Newton's equation of motion (2.47) is a set of ordinary differential equations. Although we have many sophisticated numerical techniques for solving ordinary differential equations [29], MD simulations usually use rather simple finite difference methods. This is because we have to deal with a number of molecules in the system N, and/or we have to continue computations for quite large steps M. The number of molecules N and the number of steps M sometimes exceed $N = 10^6$ and $M = 10^8$. Large N and M directly result in the increase in the computational time. We therefore prefer numerical methods as simple as possible with less degradation in accuracy. The methods commonly used are the leap-frog scheme, the velocity Verlet scheme, and Gear's predictor–corrector algorithms [1, 11]. We here explain the leap-frog scheme.

In the leap-frog scheme, the nondimensionalized Newton's equation of motion (2.47) is discretized as

$$\hat{x}_j^{(i)}(\hat{t} + \Delta\hat{t}) = \hat{x}_j^{(i)}(\hat{t}) + \Delta\hat{t}\,\hat{v}_j^{(i)}(\hat{t} + \tfrac{1}{2}\Delta\hat{t}) + O(\Delta\hat{t}^{\,3}), \tag{2.52}$$

[10] For example, it is natural that large-scale fluid flows are affected by the gravity.

$$\hat{v}_j^{(i)}(\hat{t}+\tfrac{1}{2}\Delta\hat{t}) = \hat{v}_j^{(i)}(\hat{t}-\tfrac{1}{2}\Delta\hat{t}) + \Delta\hat{t}\,\hat{f}_j^{(i)}(\hat{t}) + O(\Delta\hat{t}^{\,3}), \tag{2.53}$$

where $\hat{v}_j^{(i)}$ is the jth component of velocity of the ith molecule and $\Delta\hat{t}$ is the time step. By using the Taylor expansions, it is easy to derive Eqs. (2.52) and (2.53), and to confirm that the local truncation errors are of the order of $\Delta\hat{t}^{\,3}$. Note that $\hat{f}_j^{(i)}(\hat{t})$ in the right-hand side of Eq. (2.53) is given by

$$\hat{f}_j^{(i)}(\hat{t}) = -\sum_{\substack{k=1\\k\neq i}}^{N} \frac{\hat{x}_j^{(i)}(\hat{t}) - \hat{x}_j^{(k)}(\hat{t})}{\hat{r}_{ik}(\hat{t})}\,\hat{\phi}'(\hat{r}_{ik}(\hat{t})), \tag{2.54}$$

$$\hat{r}_{ik}(\hat{t}) = \left|\hat{\boldsymbol{x}}^{(i)}(\hat{t}) - \hat{\boldsymbol{x}}^{(k)}(\hat{t})\right|, \tag{2.55}$$

and hence $\hat{v}_j^{(i)}(\hat{t}+\frac{1}{2}\Delta\hat{t})$ can be obtained by Eq. (2.53) if $\hat{v}_j^{(i)}(\hat{t}-\frac{1}{2}\Delta\hat{t})$ and $\hat{x}_j^{(i)}(\hat{t})$ are known. After obtaining $\hat{v}_j^{(i)}(\hat{t}+\frac{1}{2}\Delta\hat{t})$, we can determine $\hat{x}_j^{(i)}(\hat{t}+\frac{1}{2}\Delta\hat{t})$ by Eq. (2.52), and the computation can be continued to the next time step. Thus, the time series of positions and velocities obtained by the leap-frog scheme (2.52) and (2.53) are shifted by the half of the time step.

In many cases, it is important and useful to monitor the value of the total energy (total Hamiltonian) (2.10), which can be written in the nondimensional form as follows:

$$\hat{\mathcal{H}}(\hat{t}) = \frac{1}{2}\sum_{i=1}^{N}\sum_{j=1}^{3}\hat{v}_j^{(i)}(\hat{t})\hat{v}_j^{(i)}(\hat{t}) + \frac{1}{2}\sum_{i=1}^{N}\sum_{\substack{k=1\\k\neq i}}^{N}\hat{\phi}\left(\hat{r}_{ik}(\hat{t})\right). \tag{2.56}$$

For the evaluation of $\hat{\mathcal{H}}(\hat{t})$, we can use

$$\hat{v}_j^{(i)}(\hat{t}) = \frac{1}{2}\left[\hat{v}_j^{(i)}(\hat{t}+\tfrac{1}{2}\Delta\hat{t}) + \hat{v}_j^{(i)}(\hat{t}-\tfrac{1}{2}\Delta\hat{t})\right] + O(\Delta\hat{t}^{\,2}). \tag{2.57}$$

The error of the order of $\Delta\hat{t}^{\,2}$ brought into $\hat{\mathcal{H}}(\hat{t})$ by the use of Eq. (2.57) may not lead to serious problems, because Eq. (2.57) is used only in the evaluation of $\hat{\mathcal{H}}$, and significant errors are caused by the accumulation of local truncation errors for a large number of computational steps.

Even if the number of molecules in the system is not so large, e.g., $N = 10^4$, the exact evaluation of $\hat{f}_j^{(i)}$ is a hard task because of the long tail of attractive force, as shown in Fig. 2.2. Since the tail of attractive force decays as $\hat{r}^{-7}$, it seems to be reasonable to cut it off at some distance $\hat{r}_{\mathrm{cut}}$ from the center of the ith molecule. Many authors have so far used $\hat{r}_{\mathrm{cut}} = 2.5$ in their MD simulations. However, the simulations of vapor–liquid interface and its neighborhood are strongly affected by the details of the numerical method, such as, the size of cut-off radius $\hat{r}_{\mathrm{cut}}$, the thickness of liquid layer, and the area of the interface [12, 26, 40]. In particular, the

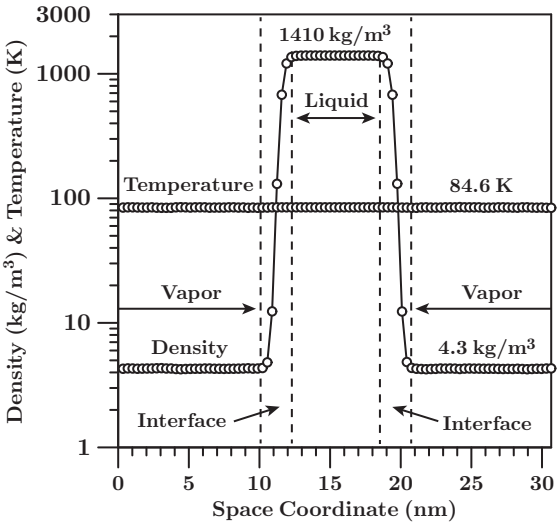

Fig. 2.3 The density and temperature in a vapor–liquid equilibrium state. In the figure, the density transition layer is shown as the interface

shorter is the cut-off radius, the lower the liquid density and the higher the vapor density. According to Refs. [12, 26, 40], to suppress artificial effects due to small $\hat{r}_{\mathrm{cut}}$, it should be larger than or at least equal to 4.4 (it corresponds to 1.5 nm for the case of argon).

Usually, the simulation is performed for a specified N molecules put in a simulation box fixed in the coordinate system. We therefore impose some boundary condition at the surface of the box. The most simple one is the periodic boundary condition [1, 11], and it enables us to avoid introducing artificial boundary conditions and to conserve the number of molecules. Needless to say, the use of the periodic boundary condition does not imply the simulation of infinitely large volume at all, even in the cases of equilibrium simulation. For example, the thickness of the vapor–liquid interface (density transition layer), as shown in Fig. 2.3 in Sect. 2.2.3 and illustrated in Fig. 2.7 in Sect. 2.4.1, is known to be a logarithmically increasing function of the area of the interface (the cross section of the simulation box) [12, 26, 40]. Furthermore, if the size of the box is not sufficiently large compared with the cut-off radius, the artificial effect of periodic boundary condition spoils the result of simulations [1, 11].

2.2.3 Example: Vapor–Liquid Equilibrium State

As an example of MD simulations, we present the distributions of averaged density and temperature of a vapor–liquid coexistence system including two interfaces in Fig. 2.3, where a planar liquid layer of monatomic molecules exists between two vapor phases of the same molecules, and the system is in an equilibrium state.

Although the simulation is performed with nondimensional variables defined in previous subsections, the dimensional density and temperature are shown in Fig. 2.3 with the use of $(\epsilon/k, \sigma) = (119.8\,\mathrm{K}, 0.341\,\mathrm{nm})$ for argon. The temperature (84.6 K) is uniform,[11] the liquid density is 1410 kg/m^3, and the vapor density is 4.3 kg/m^3, which are in agreement with known values [28] with errors less than 1%. The density profile in Fig. 2.3 shows that the vapor–liquid interface has a finite thickness. The dashed line in Fig. 2.3 denotes the edge of the bulk liquid region or bulk vapor region, where we tentatively use "bulk" to indicate that the averaged density is spatially uniform.

The details of the simulation method are as follows: The simulation box is $L_1 \times L_2 \times L_3 = 90\sigma \times 30\sigma \times 30\sigma$ nm^3, and a planar liquid layer with thickness about 7 nm is set at around $x_1 = L_1/2$ as the initial condition, and the total number of molecules is $N = 17280$. Under the periodic boundary condition, Newton's equations of motion (2.47), (2.48), (2.49), and (2.50) for N molecules are numerically solved by using the leap-frog scheme (2.52) and (2.53) with the time step $\Delta\hat{t} = 0.0005$ ($\sigma\sqrt{m/\epsilon}\Delta\hat{t} = 10^{-15}$ s) and the cut-off radius $\hat{r}_{\mathrm{cut}} = 5$ ($\sigma\hat{r}_{\mathrm{cut}} = 1.7$ nm). The number of total simulation steps is $M = 4 \times 10^8$ ($\sigma\sqrt{m/\epsilon}M\Delta\hat{t} = 4 \times 10^{-7}$ s). The first half of M simulation steps is dedicated to a relaxation process to a vapor–liquid equilibrium, and the results shown in Fig. 2.3 are evaluated from averages of samples obtained in the second half of M steps.

The evaluation of density and temperature uses Eqs. (2.18) and (2.45). Since the phenomenon considered here is one-dimensional in the macroscopic sense, the function χ defined by Eq. (2.19) should be replaced by

$$\chi^1(\boldsymbol{q}^{(i)} - \boldsymbol{x}; h) = \begin{cases} 1 & \left|q_1^{(i)} - x_1\right| \leqq h/2, \\ 0 & \left|q_1^{(i)} - x_1\right| > h/2. \end{cases} \tag{2.58}$$

Accordingly, the volume of the cube h^3 in Eqs. (2.18) and (2.45) should also be replaced by hL_2L_3 (see Fig. 2.4). The integration of any function multiplied by the probability density $F(\boldsymbol{q}, \boldsymbol{p}, t)$ with respect to $\boldsymbol{q}$ and $\boldsymbol{p}$ is naturally replaced by the summation over a large number of samples obtained in the MD simulation.

The errors introduced by the cut-off of the intermolecular force are illustrated in Fig. 2.5a, where the error is defined by the difference of $\left|\boldsymbol{f}^{(i)}\right|$ with $\hat{r}_{\mathrm{cut}}$ from $\left|\boldsymbol{f}^{(i)}\right|$ with $\hat{r}_{\mathrm{cut}} = 10$ for some ith molecule at some instant t. From the figure, we can approximately estimate that the error of molecules in the bulk liquid phase decreases with $10^{-3\hat{r}_{\mathrm{cut}}/4}$ as $\hat{r}_{\mathrm{cut}}$ increases, and that of molecules at the edge of the bulk liquid phase decreases more slowly with $10^{-\hat{r}_{\mathrm{cut}}/4}$. The molecular motions in the vicinity of the interface is therefore affected by the size of cut-off radius of intermolecular potential strongly. The use of a small cut-off radius results in an equilibrium system with a high vapor density and a low liquid density [12, 26, 40].

[11] The triple point temperature is 83.8 K for argon [28].

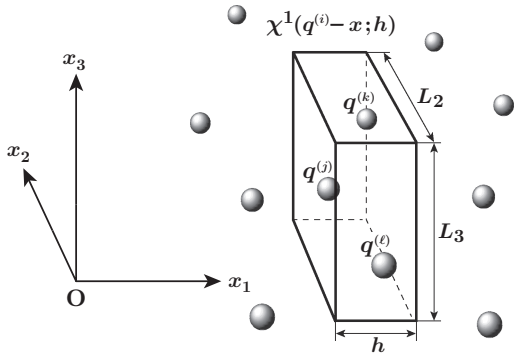

Fig. 2.4 The function χ^1 for spatially one-dimensional problems in the macroscopic sense

Figure 2.5b illustrates how the system size (number of total molecules N) affects the total Hamiltonian $\hat{\mathcal{H}}$ defined by (2.56) and numerical errors in $\hat{\mathcal{H}}$. Here, the error is defined by three times the standard deviation of $\hat{\mathcal{H}}$. In the figure, four systems with different N (4320, 17280, 69588, 286487) are compared, for which we use the same leaf-frog scheme with the same cut-off radius $\hat{r}_{\rm cut} = 5$ and the same time step $\Delta\hat{t} = 0.0005$, and different simulation boxes: $(L_1/\sigma, L_2/\sigma, L_3/\sigma) = (90, 15, 15)$ for $N = 4320$, $(90, 30, 30)$ for $N = 17280$, $(150, 60, 60)$ for $N = 69588$, $(390, 120, 120)$ for $N = 286487$. In our vapor–liquid two-phase systems, almost

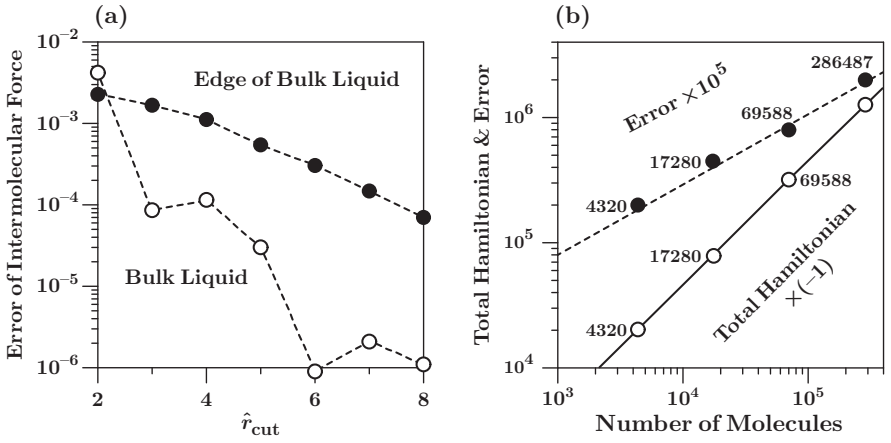

Fig. 2.5 (**a**) The difference between the intermolecular force with various cut-off $\hat{r}_{\rm cut}$ and that with $\hat{r}_{\rm cut} = 10$ is shown as a measure of error in the intermolecular force, where the *open circle* denotes the force on some molecule in the bulk liquid phase and the *closed circle* denotes that on some molecule at the edge of the bulk liquid phase. (**b**) The relation between the error in the total Hamiltonian and the number of molecules in the system. The *open circles* are $\hat{\mathcal{H}} \times (-1)$ and the *closed circles* are three times the standard deviation of $\hat{\mathcal{H}} \times 10^5$. The number near the symbol denotes the total number of molecules in the system, N. The *solid line* is a line of slope 1 and the *dashed line* slope 1/2

80% of $\hat{\mathcal{H}}$ is the potential energy of molecules in liquid and hence $\hat{\mathcal{H}}$ is substantially determined by the number of molecules in the liquid layer. This is the reason why $\hat{\mathcal{H}}$ in Fig. 2.5b is proportional to N. The important conclusion from Fig. 2.5b is that if $\hat{\mathcal{H}} \propto N$, then the error $\propto \sqrt{N}$. Theoretically, $\hat{\mathcal{H}}$ should be constant in NVE simulations as well as in an isolated system, and therefore, the fluctuation in $\hat{\mathcal{H}}$ is purely numerical. Figure 2.5b suggests that the numerical error in $\hat{\mathcal{H}}$ also is governed by the central limit theorem.[12]

2.3 Kinetic Theory of Gases

The kinetic theory is a microscopic theory of processes in systems not in statistical equilibrium [24]. A kinetic boundary condition means a boundary condition for a kinetic equation, the governing equation of a kinetic theory, such as the Boltzmann equation [35], the Vlasov equation for plasma [9], the Enskog equation for dense gases [31].

In contrast to the well-established kinetic theory of gases, the rigorous kinetic theory of liquids is considerably complicated [5], and its formidable mathematical difficulties impede reducing and interpreting the formal solutions. The origin of difficulties is clearly apparently random multi-body interactions of molecules in liquids. On the other hand, the kinetic theory of gases based on the Boltzmann equation, which is a mainstay of this book, deals with dilute gases in the sense that the three-body interaction of gas molecules does not occur. As a result, the kinetic theory of gases permits us to obtain a number of fruits from it, although the exact kinetic theory of gases is still mathematically difficult.

In the context of this book, however, the random multi-body interactions of liquid molecules are not necessarily an obstacle for our purpose. It allows us to expect that the liquid is in a local equilibrium state everywhere except for the interface because of a sufficiently rapid relaxation to equilibrium due to frequent multi-body interactions of molecules in liquids. Once the local equilibrium in a liquid is admitted, we can focus our attention to the behavior of gas molecules under the given macroscopic condition of the liquid. Strictly speaking, if the evaporation or condensation at the interface is not so weak, the assumption of local equilibrium in the liquid may not be accepted uncritically. For example, if the heat flux across the interface due to the evaporation or condensation is fairly large, the liquid near the interface may deviate from a local equilibrium state. If the liquid near the interface is not in a local equilibrium state, we cannot specify the macroscopic condition of the liquid, which is necessary to analyze the vapor flow separately by the kinetic theory of gases. In this book, we therefore confine ourselves to the case of weak evaporation/condensation state, the precise definition of which is given in Sects. 2.5.1 and 2.5.2. Although we determine the molecular motions in the liquid in a rigorous way of the MD

[12] It is easy to confirm that the probability density of numerically obtained $\hat{\mathcal{H}}$ approaches a Gaussian with the increase in N.

simulation, some constraints are still imposed on the bulk of the liquid, and we do not pursue the kinetic theory of liquids.

2.3.1 Boltzmann Equation

For the present, we confine ourselves to the gases of monatomic molecules.

In the kinetic theory of gases, the only unknown microscopic variable is the velocity distribution function of gas molecules, $f(\boldsymbol{x}, \boldsymbol{\xi}, t)$, defined by

$$m\,\mathrm{d}N = f(\boldsymbol{x}, \boldsymbol{\xi}, t)\,\mathrm{d}\boldsymbol{x}\,\mathrm{d}\boldsymbol{\xi}, \tag{2.59}$$

where $\mathrm{d}N$ in the left-hand side denotes the number of molecules in a volume element $\mathrm{d}\boldsymbol{x}\,\mathrm{d}\boldsymbol{\xi} = \mathrm{d}x_1\mathrm{d}x_2\mathrm{d}x_3\mathrm{d}\xi_1\mathrm{d}\xi_2\mathrm{d}\xi_3$ centered at $(\boldsymbol{x}, \boldsymbol{\xi})$ in the 6-dimensional space of the position $\boldsymbol{x}$ and the velocity $\boldsymbol{\xi}$ of a molecule [35] (N signifies the number of molecules). The governing equation for f is the Boltzmann equation,

$$\frac{\partial f}{\partial t} + \xi_j \frac{\partial f}{\partial x_j} = J(f), \tag{2.60}$$

where $J(f)$ in the right-hand side represents the effects of the intermolecular collisions. Here and hereafter the Einstein summation convention is used, e.g.,

$$\xi_j \frac{\partial f}{\partial x_j} = \sum_{j=1}^{3} \xi_j \frac{\partial f}{\partial x_j}, \tag{2.61}$$

(see Appendix A at the end of this book). Furthermore, the notation of the jth component of a vector $\boldsymbol{a}$, a_j, will be used without notice.

Once given the velocity distribution function $f(\boldsymbol{x}, \boldsymbol{\xi}, t)$, the macroscopic variables are evaluated by

$$\rho = \int f\,\mathrm{d}\boldsymbol{\xi}, \quad v_i = \frac{1}{\rho}\int \xi_i f\,\mathrm{d}\boldsymbol{\xi}, \quad T = \frac{1}{3\rho R}\int (\xi_j - v_j)^2 f\,\mathrm{d}\boldsymbol{\xi}, \tag{2.62}$$

where ρ is the gas density, v_i is the gas velocity, and T is the gas temperature. The definitions of stress tensor and heat flux have already been given by Eqs. (2.41) and (2.42) in Sect. 2.1.3. The gas pressure p and the internal energy e are given by $p = \rho RT$ and $e = (3R/2)T$, respectively.[13]

The collision term $J(f)$ for the molecules with a spherically symmetric intermolecular potential with a finite influence range d_m is given by a five-fold integral of f [35],

[13] The relations $p = \rho RT$ and $e = (3R/2)T$ do not imply that the gas is in a (local) equilibrium state. They are formal extensions to nonequilibrium states, as well as the definition of temperature T.

$$J(f) = \frac{1}{m} \int_{\text{all } \alpha_i,\, \text{all } \xi_{i*}} (f' f'_* - f f_*)\, B \, \mathrm{d}\Omega(\boldsymbol{\alpha}) \, \mathrm{d}\boldsymbol{\xi}_*, \tag{2.63}$$

where

$$f = f(x_i, \xi_i, t),\ f' = f(x_i, \xi'_i, t),\ f_* = f(x_i, \xi_{i*}, t),\ f'_* = f(x_i, \xi'_{i*}, t), \tag{2.64}$$

$$\xi'_i = \xi_i + \alpha_i \alpha_j (\xi_{j*} - \xi_j),\ \xi'_{i*} = \xi_{i*} - \alpha_i \alpha_j (\xi_{j*} - \xi_j), \tag{2.65}$$

$$B = B\left(\frac{\alpha_j (\xi_{j*} - \xi_j)}{|\boldsymbol{\xi}_* - \boldsymbol{\xi}|}, |\boldsymbol{\xi}_* - \boldsymbol{\xi}| \right), \tag{2.66}$$

and $\boldsymbol{\alpha}$ is a unit vector expressing the variation of the direction of molecular velocity just before and after the collision, $\mathrm{d}\Omega(\boldsymbol{\alpha})$ is the solid-angle element in the direction of $\boldsymbol{\alpha}$, and the functional form of B is determined by the intermolecular force; for example, $B = d_m^2 |\alpha_j (\xi_{j*} - \xi_j)|/2$ for a gas consisting of hard-sphere molecules with diameter d_m [35].

The mean free path of gas molecules, ℓ, is defined as the product of the molecular average speed $\overline{\xi} = (8RT/\pi)^{1/2}$ and the inverse of the mean collision frequency $\overline{\nu}_c$ [35],

$$\ell = \frac{\overline{\xi}}{\overline{\nu}_c}, \tag{2.67}$$

where the mean collision frequency[14]

$$\overline{\nu}_c = \frac{1}{\rho m} \int f(\boldsymbol{\xi}) f(\boldsymbol{\xi}_*)\, B \, \mathrm{d}\Omega(\boldsymbol{\alpha}) \, \mathrm{d}\boldsymbol{\xi} \, \mathrm{d}\boldsymbol{\xi}_*, \tag{2.68}$$

is an average of the collision frequency of a molecule with velocity $\boldsymbol{\xi}$

$$\nu_c(\boldsymbol{\xi}) = \frac{1}{m} \int f(\boldsymbol{\xi}_*)\, B \, \mathrm{d}\Omega(\boldsymbol{\alpha}) \, \mathrm{d}\boldsymbol{\xi}_*. \tag{2.69}$$

The integrations are taken over 6-dimensional space of $(\boldsymbol{\xi}, \boldsymbol{\xi}_*)$ in Eq. (2.68) and over 3-dimensional space of $\boldsymbol{\xi}_*$ in Eq. (2.69). When the velocity distribution function f is the Maxwellian (the Maxwell distribution function) with constant ρ_0, T_0, and v_{0i},

$$f_M(\boldsymbol{\xi}) = \frac{\rho_0}{(2\pi RT_0)^{3/2}} \exp\left[-\frac{(\xi_i - v_{0i})^2}{2RT_0} \right], \tag{2.70}$$

[14] The inverse of the mean collision frequency is called the mean free time.

the mean collision frequency $\overline{\nu}_c$ defined by Eq. (2.68) can be evaluated as

$$\overline{\nu}_c = 4d_m^2(\pi RT_0)^{1/2}\frac{\rho_0}{m}, \tag{2.71}$$

where ρ_0/m is the number density of molecules and, as mentioned earlier, d_m is the radius of the influence range of the intermolecular force (not restricted to the diameter of a hard-sphere molecule) [35]. The mean free path is then given by

$$\ell = \frac{1}{\sqrt{2}\pi d_m^2(\rho_0/m)}. \tag{2.72}$$

Here, we should comment on the fundamental framework of the kinetic theory of gases based on the Boltzmann equation. The collision term of the Boltzmann equation only considers the binary collision of molecules. Mathematically, this is a situation where $N \to \infty$ and $d_m \to 0$ with Nd_m^2 fixed. This is called the Grad–Boltzmann limit [35]. In this limit, we have $Nd_m^3 \to 0$, and this means that the gas is an ideal gas. The Nd_m^2 corresponds to the inverse of the mean free path of gas molecules,[15] and it can be arbitrarily small or large as far as it is kept at a fixed value in the limiting process of $N \to \infty$ and $d_m \to 0$. The wide applicability of the Boltzmann equation from atmospheric to very low pressures is therefore the consequence of the Grad–Boltzmann limit. In the right-hand side of Eq. (2.63), one can see a factor m^{-1}, which tends to infinity as m tends to zero. The collision term is, however, always bounded because the function B has a factor d_m^2. In other words, it is implicitly assumed that the mass of a molecule $m \to 0$ as $N \to \infty$ with keeping Nm fixed at a finite value, as it should be. This is the reason why we define the velocity distribution function by Eq. (2.59). In many literature, however, the velocity distribution function is defined by f/m, which is infinite in the Grad–Boltzmann limit.

In addition to the hard-sphere model, the following model is widely used for the collision term of the Boltzmann equation (2.60):

$$J(f) = A_c\rho(f_e - f), \tag{2.73}$$

$$f_e = \frac{\rho}{(2\pi RT)^{3/2}}\exp\left[-\frac{(\xi_j - v_j)^2}{2RT}\right], \tag{2.74}$$

where A_c is a constant, f_e is the local Maxwellian with density ρ, velocity v_j, and temperature T defined by Eq. (2.62). The Boltzmann equation with the collision term (2.73) with Eq. (2.74) is called the Boltzmann–Krook–Welander (BKW) equation [35]. Since ρ, v_j, and T in Eqs. (2.73) and (2.74) are given by the integrals of

[15] Precisely, the mean free path corresponds to $1/(n_0 d_m^2)$, where n_0 is a characteristic number density of gas molecules, as shown by Eq. (2.72).

unknown function f as shown in Eq. (2.62), the BKW equation is a highly nonlinear integro-differential equation.

The constant A_c in Eq. (2.73) is related to the mean free path ℓ of molecules in the gas in an equilibrium state with density ρ and temperature T as

$$\ell = \frac{(8RT/\pi)^{1/2}}{A_c \rho}, \tag{2.75}$$

where $A_c \rho$ is the collision frequency (ν_c) of molecules described by the BKW equation. That is, the collision frequency of molecules described by the BKW equation is independent of the molecular velocity $\boldsymbol{\xi}$ [see Eqs. (2.68) and (2.69)], and hence $\nu_c = \overline{\nu}_c$.

The BKW equation shares the important properties in the kinetic theory of gases with the standard Boltzmann equation with the collision term (2.63), (2.64), (2.65), and (2.66): (i) the Maxwellian (2.70) is the solution expressing the equilibrium state, where ρ_0, v_{0i}, and T_0 are constants, (ii) the same conservation equations for macroscopic variables can be derived as those from the standard Boltzmann equation, and (iii) the Boltzmann H-theorem[16] holds [35]. By many theoretical and numerical studies, it has been confirmed that not only qualitatively but also quantitatively similar results are obtained for the BKW equation and the standard Boltzmann equation, except that the BKW equation gives the Prandtl number equal to unity [35].

Furthermore, the BKW equation has an advantage that two components of molecular velocity can be eliminated in spatially one-dimensional problems [35], and this considerably reduces the computational cost in simulation studies. The Gaussian–BGK Boltzmann equation [2] also has the same advantage, and as a result, we have obtained several substantial results in the analysis of shock-tube experiment for the condensation coefficients of water and methanol, as shown in Chap. 3.

---

[16] The Boltzmann H-theorem corresponds to the entropy inequality extended to nonequilibrium states [35]. The theorem states that the H function or the integral $\overline{H}$ of H function over a domain D,

$$H = \int f \ln(f/c)\, \mathrm{d}\boldsymbol{\xi} \quad \text{or} \quad \overline{H} = \int_D H\, \mathrm{d}\boldsymbol{x},$$

never increases by an inequality

$$\frac{\mathrm{d}\overline{H}}{\mathrm{d}t} - \int_{\partial D} (H_i - H v_{wi}) n_i\, \mathrm{d}S = \int_D \left(\int [1 + \ln(f/c)] J(f)\, \mathrm{d}\boldsymbol{\xi} \right) \mathrm{d}V \leqq 0,$$

if $(H_i - H v_{wi}) n_i = 0$ on the boundary ∂D, where c is a constant to make f/c dimensionless and

$$H_i = \int \xi_i f \ln(f/c)\, \mathrm{d}\boldsymbol{\xi}.$$

2.3.2 Boundary Condition for the Boltzmann Equation

The gas molecules impinging on the surface of solid or liquid are scattered by some rule. That is, the velocity distribution of molecules leaving the boundary should be regulated by some rule other than the molecular interaction law in the gas. This is the boundary condition for the Boltzmann equation and called the kinetic boundary condition.

In the case of a solid boundary [see Fig. 2.6a], the commonly used one is the diffuse-reflection condition [35],

$$f(\boldsymbol{x}, \boldsymbol{\xi}, t) = \frac{\rho_w}{[2\pi R T_w(\boldsymbol{x}, t)]^{3/2}} \exp\left\{-\frac{[\xi_i - v_{wi}(\boldsymbol{x}, t)]^2}{2RT_w(\boldsymbol{x}, t)}\right\}, \tag{2.76}$$

for molecules leaving the boundary with the velocity $\boldsymbol{\xi}$ satisfying

$$\boldsymbol{\xi} \cdot \boldsymbol{n}(\boldsymbol{x}, t) > \boldsymbol{v}_w(\boldsymbol{x}, t) \cdot \boldsymbol{n}(\boldsymbol{x}, t), \tag{2.77}$$

at a point $\boldsymbol{x}$ on the surface of the boundary and at a time t, where $T_w(\boldsymbol{x}, t)$ and $\boldsymbol{v}_w(\boldsymbol{x}, t)$ are respectively the temperature and velocity at the point on the surface of the boundary, $\boldsymbol{n}(\boldsymbol{x}, t)$ is the unit vector normal to the surface and pointing to the gas phase, and

$$\rho_w = -\left[\frac{2\pi}{RT_w(\boldsymbol{x}, t)}\right]^{1/2} \times \int_{\xi_j n_j(\boldsymbol{x},t) < v_{wj}(\boldsymbol{x},t) n_j(\boldsymbol{x},t)} \left[\xi_j - v_{wj}(\boldsymbol{x}, t)\right] n_j(\boldsymbol{x}, t) f(\boldsymbol{x}, \boldsymbol{\xi}, t)\, \mathrm{d}\boldsymbol{\xi}. \tag{2.78}$$

The diffuse-reflection condition represents the situation that all the molecules impinging on the boundary are isotropically emitted from the boundary after the full adaptation to the velocity and temperature of the boundary in an infinitesimal time interval. From the diffuse-reflection condition (2.76), (2.77), and (2.78), it can immediately be confirmed that the mass flux across the boundary is equal to zero.

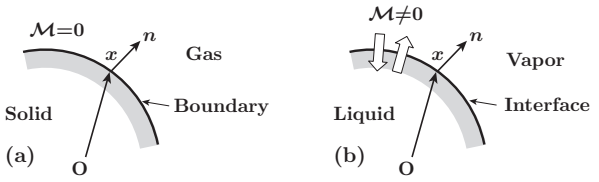

Fig. 2.6 (**a**) The solid boundary and the unit normal vector pointing to the gas phase. (**b**) The vapor–liquid interface and the unit normal vector pointing to the vapor phase

In the case that the boundary is a vapor–liquid interface [see Fig. 2.6b], the simplest one is the complete-condensation condition [35],

$$f(\boldsymbol{x}, \boldsymbol{\xi}, t) = \frac{\rho^*}{[2\pi RT_w(\boldsymbol{x}, t)]^{3/2}} \exp\left\{-\frac{[\xi_i - v_{wi}(\boldsymbol{x}, t)]^2}{2RT_w(\boldsymbol{x}, t)}\right\}, \tag{2.79}$$

for molecules leaving the boundary with the velocity satisfying Eq. (2.77), where ρ^* is the saturated vapor density at temperature $T_w(\boldsymbol{x}, t)$. The mass flux $\mathcal{M}$ across the interface is then given by

$$\mathcal{M}(\boldsymbol{x}, t) = (\rho^* - \rho_w)\sqrt{\frac{RT_w(\boldsymbol{x}, t)}{2\pi}}, \tag{2.80}$$

where Eq. (2.78) is used. The right-hand side of Eq. (2.79) is the same form as the Maxwell distribution in the vapor–liquid equilibrium state of uniform temperature T_w and uniform velocity $\boldsymbol{v}_w$. In the equilibrium state, the velocity distribution function of impinging molecules, appearing in the integrand of Eq. (2.78), is equal to the Maxwellian, and hence ρ_w defined by Eq. (2.78) is equal to ρ^*, which yields $\mathcal{M} = 0$.

The situation represented by the complete-condensation condition may be explained as follows: (i) all the molecules impinging on the interface are adsorbed to the interface; (ii) it is impossible or meaningless to distinguish which molecule leaving the boundary is reflected at the boundary or comes from the inside of the interface; (iii) the velocity distribution of molecules leaving the interface is independent of the vapor and solely determined by the interface properties, ρ^*, T_w, and $\boldsymbol{v}_w$.

Both the diffuse-reflection and complete-condensation conditions have the same Maxwellian-like functional form with respect to the molecular velocity $\boldsymbol{\xi}$. If we assume that the $\boldsymbol{\xi}$-dependence of a boundary condition is unchanged irrespective of the gas condition, the Maxwellian-like functional form is essential because the boundary-value problem of the Boltzmann equation has an equilibrium solution of Maxwellian.

Since the situations of diffuse-reflection and complete-condensation conditions are compatible and they have the same Maxwellian-like functional form with respect to $\boldsymbol{\xi}$, another type of boundary condition can be considered [35]:

$$f(\boldsymbol{x}, \boldsymbol{\xi}, t) = \frac{\alpha_e\rho^* + (1 - \alpha_c)\rho_w}{[2\pi RT_w(\boldsymbol{x}, t)]^{3/2}} \exp\left\{-\frac{[\xi_i - v_{wi}(\boldsymbol{x}, t)]^2}{2RT_w(\boldsymbol{x}, t)}\right\}, \tag{2.81}$$

with Eq. (2.78) for molecules leaving the boundary with the velocity satisfying Eq. (2.77), where α_e ($0 \leqq \alpha_e \leqq 1$) and α_c ($0 \leqq \alpha_c \leqq 1$) are called the evaporation coefficient and condensation coefficient, respectively. This mixed-type boundary condition (2.81) has also widely been used so far, and is our target in this book.

In the kinetic boundary condition (2.81), we assume that the information of molecules impinging on the interface is contained in $(1-\alpha_c)\rho_w$ only, and α_e in the right-hand side of Eq. (2.81) is independent of molecules impinging on the interface. Under these assumptions, the α_e part in Eq. (2.81), i.e., the complete-condensation condition multiplied by α_e, is unchanged even if there are no molecules impinging on the interface. That is, the α_e part does not include the molecules reflected at the interface, and hence α_e is named the evaporation coefficient. The α_e part in Eq. (2.81) is studied by a nonequilibrium MD simulation in Sect. 2.4.1. On the other hand, the $(1-\alpha_c)$ part, i.e., the diffuse-reflection condition multiplied by $(1-\alpha_c)$, may be regarded as the reflection part and the remaining α_c fraction of ρ_w may be considered to be condensed on the interface. Hence, α_c is called the condensation coefficient. The condensation coefficient α_c and Eq. (2.81) itself are studied in Sect. 2.4.2 by a nonequilibrium MD simulation.

Based upon the kinetic boundary condition (2.81), the mass flux across the interface is given by

$$\mathcal{M} = (\alpha_e \rho^* - \alpha_c \rho_w)\sqrt{\frac{RT_w(\boldsymbol{x}, t)}{2\pi}}. \tag{2.82}$$

This formula will be repeatedly utilized in this book.

The formulation of the boundary-value problem for vapor adjacent to a vapor–liquid interface is completed by the Boltzmann equation (2.60), the boundary condition at the interface, Eqs. (2.81), (2.77), (2.78), and the boundary condition at infinity.

We assume that the evaporation or condensation is sufficiently weak so that we can expect that the liquid is in a local equilibrium state. This allows us to determine the temperature field and velocity field in the liquid phase by the equations of fluid dynamics (see Appendix B at the end of this book). The temperature $T_w(\boldsymbol{x}, t)$ and velocity $v_{wi}(\boldsymbol{x}, t)$ at the interface are thus determined without relying on the kinetic theory of liquids. Then, we can solve the boundary-value problem of the Boltzmann equation. Now, we have made all sorts of preparations for tackling our main problem.

2.4 Kinetic Boundary Condition

The first topic of our main problem in this chapter is to establish the kinetic boundary condition at the vapor–liquid interface by the method of molecular dynamics (MD) simulation. In Sect. 2.3.2, we have introduced the boundary condition (2.81) as a widely used one. However, the derivation of (2.81) has not been accomplished neither from the kinetic theories of gases and liquids nor from the Liouville equation (2.16). Until the MD studies on (2.81) were performed [16–18], it has been just a mathematical model. In Sect. 2.4.1, according to Refs. [16–18], we firstly construct the α_e part of Eq. (2.81) and determine the values of α_e for argon, water, and methanol by specially devised nonequilibrium MD simulations. Then, in Sect. 2.4.2,

by using further devised MD simulation of nonequilibrium states, we formulate the kinetic boundary condition at the vapor–liquid interface, the result of which is substantially equal to Eq. (2.81) if the condensation mass flux across the interface is not so large.

2.4.1 Evaporation into Vacuum

In Sect. 2.3.2, the α_e part of Eq. (2.81) is assumed to be independent of the molecules impinging on the interface and unchanged even if no molecules impinge on the interface. We therefore consider a situation that all vapor molecules near the interface have the velocities in the direction of leaving the interface. This can be realized in a molecular simulation by eliminating the molecules impinging on the interface, and we call this type of simulation the MD simulation of evaporation from the interface into a virtual vacuum [16, 17]. Note that the vapor density near the interface cannot be zero in reality, and hence we call this situation the virtual vacuum. From the samples obtained by the simulation, we can directly construct the velocity distribution function of molecules evaporating from the interface, and thereby investigating the functional form of the velocity distribution function. Such an MD simulation of evaporation into vacuum has first been performed by Anisimov et al. [3].

The simulation is started from an equilibrium vapor–liquid two-phase system as shown in Fig. 2.3 [16, 17]. Although the equations solved are Newton's equations of motion (2.47), (2.48), (2.49), and (2.50) in the nondimensional form, we present the results in the dimensional forms with the use of $(\epsilon/k, \sigma) = (119.8\ \mathrm{K}, 0.341\ \mathrm{nm})$ for argon. The leap-frog method with the time step 10^{-15} s and the cut-off radius 1.5 nm (4.4 σ) are used.

The evaporation into a virtual vacuum is actualized by eliminating vapor molecules in a region that is a few multiples of a thickness of interface distant from the center of the interface, where the center of the interface x_0 and the thickness of the interface δ are defined by

$$x_0 = \rho^{-1}\left(\frac{\rho_L + \rho_V}{2}\right), \tag{2.83}$$

$$\delta = \rho^{-1}\left(\rho_V + \frac{\rho_L - \rho_V}{10}\right) - \rho^{-1}\left(\rho_L - \frac{\rho_L - \rho_V}{10}\right), \tag{2.84}$$

where ρ_L and ρ_V are the density of the liquid and vapor near the interface, and ρ^{-1} is the inverse function of $\rho(x)$ (x is the space coordinate normal to the interface, which is a plane in the macroscopic sense). The thickness δ defined by Eq. (2.84) is called the 10–90 thickness (see Fig. 2.7). Since the evaporating molecules carry the energy from the liquid, the temperature of liquid drops with the time goes on. To maintain the temperature in the liquid, we apply the temperature control by the velocity scaling method [1], and thus the evaporation phenomenon observed on the coordinate fixed at the interface can be regarded as a steady state. The distance where the vapor molecules are eliminated and the region where the temperature

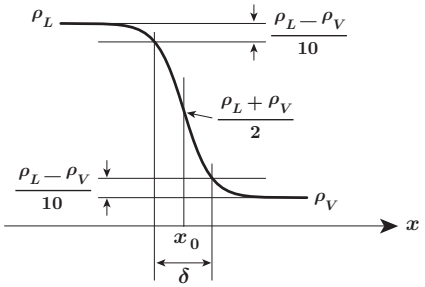

Fig. 2.7 The density profile (*bold curve*), the center of the interface x_0, and the 10–90 thickness δ of the density transition layer

control is applied are carefully examined and chosen appropriately [16]. However, by the temperature control, the temperature in a bulk liquid region is rendered to be uniform. The simulation may therefore be an approximation for the case that the temperature gradient in the bulk liquid phase, which is necessarily generated by the heat flux due to evaporation, is sufficiently small.

Figure 2.8 shows the averaged molecular mass fluxes in the simulation of evaporation into the virtual vacuum, where $X = (x - x_0)/\delta$ is a normalized space coordinate normal to the interface and measured from the center of the interface, and the molecular mass fluxes are averaged with respect to time on the coordinate fixed at the interface.[17] The molecules are eliminated at $X = 4$. The liquid temperature controlled by the velocity scaling is shown in the figure. The angle brackets $\langle \cdots \rangle$ in Fig. 2.8 represent a long-time average. The averaged mass flux $\langle \mathcal{M} \rangle$ shown in the figure is defined by the time average of the molecular mass flux $\mathcal{M}$

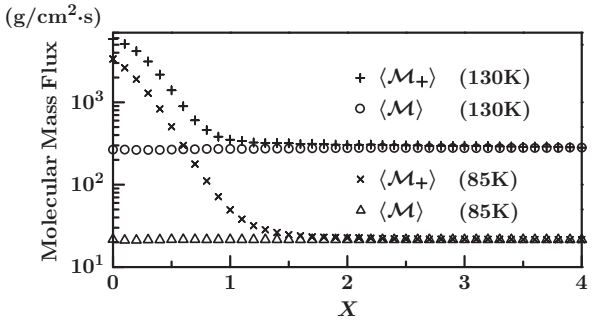

Fig. 2.8 The molecular mass fluxes in the simulation of evaporation into the virtual vacuum [16]. The liquid temperature controlled by the velocity scaling is shown in the figure. Here, the *angle brackets* represent a long-time average

[17] The center of the interface x_0 is almost constant on the coordinate fixed to the interface in spite of the backward movement of interface due to evaporation.

$$\mathcal{M}(\boldsymbol{x},t)=\frac{1}{L_2L_3h}\sum_{i=1}^{N}\int\chi^1(\boldsymbol{q}^{(i)}-\boldsymbol{x},h)p_j^{(i)}n_jF(\boldsymbol{q},\boldsymbol{p},t)\,\mathrm{d}\boldsymbol{q}\,\mathrm{d}\boldsymbol{p},\tag{2.85}$$

which is the one-dimensional counterpart of Eq. (2.20), χ^1 is defined by Eq. (2.58), and n_j is the unit vector normal to the interface and pointing to the vapor phase. Another averaged mass flux $\langle\mathcal{M}_+\rangle$ is defined by the time average of the molecular mass flux $\mathcal{M}_+$

$$\mathcal{M}_+(\boldsymbol{x},t)=\frac{1}{L_2L_3h}\sum_{\substack{i=1\\ p_j^{(i)}n_j>0}}^{N}\int\chi^1(\boldsymbol{q}^{(i)}-\boldsymbol{x},h)p_j^{(i)}n_jF(\boldsymbol{q},\boldsymbol{p},t)\,\mathrm{d}\boldsymbol{q}\,\mathrm{d}\boldsymbol{p},\tag{2.86}$$

which gives the mass flux of molecules moving in the positive X direction.

As shown in Fig. 2.8, in the region $X\lesssim 1$, the region very close to the interface, the density is not low, and hence the molecular interactions frequently happen. The difference between $\langle\mathcal{M}\rangle$ and $\langle\mathcal{M}_+\rangle$ means that there exist some molecules moving in the negative X direction. In the region $X\gtrsim 2$, the difference of the two fluxes vanishes and all molecules are evaporating into the virtual vacuum.

The velocity distribution function can be constructed according to its definition Eq. (2.59), and the results are shown in Fig. 2.9, where the normalized velocity distribution functions of the normalized molecular velocity $(\zeta_x,\zeta_y,\zeta_z)=(\xi_x,\xi_y,\xi_z)/\sqrt{2RT_L}$ are plotted and the temperature of the liquid controlled by velocity scaling T_L is also shown.[18] The velocity component normal to the interface is signified by the open circle.

At $X=0$, as shown in Fig. 2.9a, d, the velocity distribution function is the Maxwellian with the temperature T_L. Although $X=0$ is not the bulk liquid phase but the center of the interface, the normalized velocity distribution of molecules is the same as that in the equilibrium state. However, at $X=2$, the profiles of distribution of velocity component normal to the interface, ζ_x, are distorted as shown in Fig. 2.9c, e, which clearly means that the number of molecules with negative ζ_x decreases. In the case that $X=4$ and $T_L=85$ K, the distribution of $\zeta_x>0$ is almost equal to the half part of the one-dimensional Maxwellian with the temperature T_L and zero mean velocity, and the distribution of the other components are unchanged from those at $X=0$. That is, the velocity distribution of molecules evaporating into the virtual vacuum has the same functional form as that of Eq. (2.81) at $T_L=85$ K. On the other hand, at $T_L=130$ K, a significant amount of molecules have the velocity of $\zeta_x<0$ even at $X=4$. This means that, when the temperature of the liquid is high, the vapor density of molecules evaporating into the virtual vacuum is also high, and hence the molecular interaction in the vapor phase cannot be neglected.

[18] In Eq. (2.81), we used the symbol T_w for the temperature at the surface of the liquid phase.

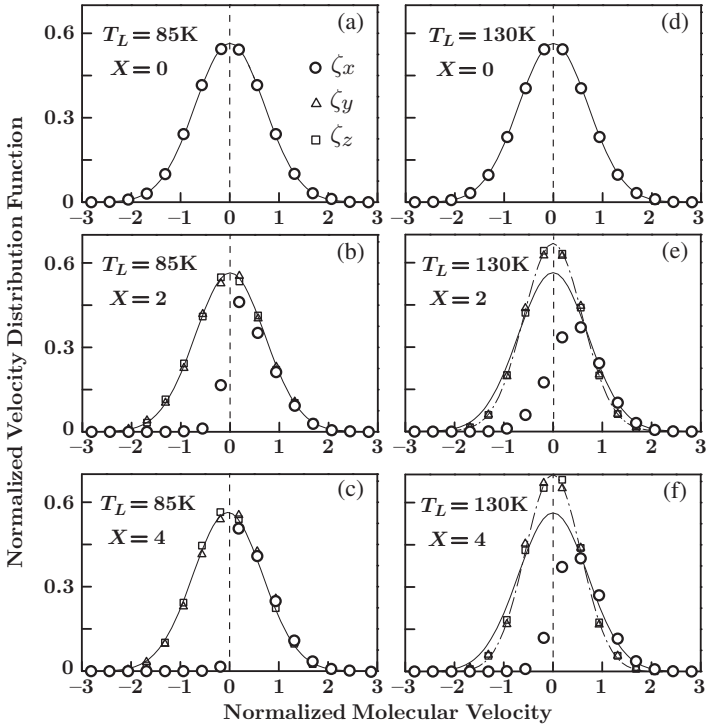

Fig. 2.9 The velocity distribution functions at $X = 0, 2, 4$ [16]. The abscissa of the figure is the normalized molecular velocity $\zeta_j = \xi_j/\sqrt{2RT_L}$ $(j = x, y, z)$, where T_L is the temperature of the liquid controlled by velocity scaling

In this case, it is impossible to realize the situation that all vapor molecules near the interface have the velocities in direction of leaving the interface. Note that the mean free path of the vapor molecules in the equilibrium at $T = 130$ K is about $2\sigma \approx 2d_m$, and hence the vapor is not in the Grad–Boltzmann limit.

2.4.2 Evaporation Coefficient

Thus, the velocity distribution function of molecules evaporating from the interface into the virtual vacuum is obtained by the MD simulation, and its functional form is found to be the half part of the Maxwellian with liquid temperature T_L and zero mean velocity, if T_L is not so high or if the vapor density is sufficiently low so that the gas may be regarded to be in the Grad–Boltzmann limit. That is, the functional form of the α_e part of Eq. (2.81), which is independent of the molecules impinging on the interface, is validated by the MD simulation. Once admitted the α_e part of Eq. (2.81), by considering the situation that $\rho_w = 0$ in Eq. (2.81), and applying Eq. (2.82), we have

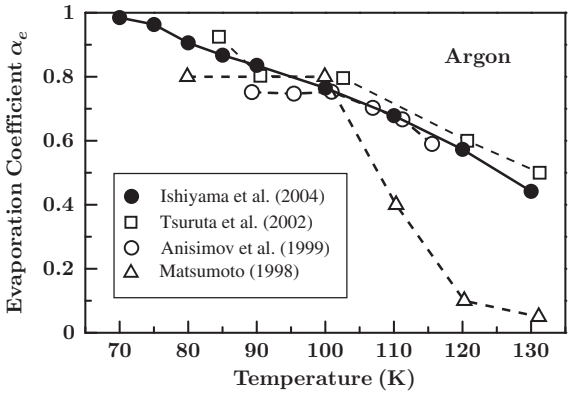

Fig. 2.10 Evaporation coefficient for argon [16] and the comparison with those obtained by other authors [3, 25, 41]

$$\langle \mathcal{M}_+ \rangle = \alpha_e \rho^* \left(\frac{RT_L}{2\pi} \right)^{1/2} . \tag{2.87}$$

The left-hand side of Eq. (2.87) has already been evaluated in the simulation as shown in Fig. 2.8, and the saturated vapor density ρ^* can be calculated from the Clausius–Clapeyron equation [30] or the equilibrium MD simulation as shown in Sect. 2.2.3. The values of the evaporation coefficient α_e can thus be determined and the results are plotted in Fig. 2.10. In the figure, the evaporation coefficient for T_L below the triple point temperature are also shown, where the sublimation occurs from the vapor–solid interface. Since the Lennard-Jones potential is not suitable for the vapor–solid equilibrium state, we have used the Dymond–Alder potential for the temperature range of sublimation [10, 16].

As can be seen from Fig. 2.10, the evaporation coefficient α_e is a decreasing function of liquid temperature, and it is almost unity at slightly below the triple point temperature. We here remark that the left-hand side of Eq. (2.87), $\langle \mathcal{M}_+ \rangle$, is evaluated by the MD simulation formulated in a nondimensional form, and hence the obtained $\langle \mathcal{M}_+ \rangle$ is applicable to other species of molecules, for which the Lennard-Jones 12-6 potential is effective, e.g., Ne, Kr, and so on. The evaporation coefficient of other species of molecules can therefore be evaluated by using $\langle \mathcal{M}_+ \rangle$ obtained here and the saturated vapor density ρ^* of the species of molecules.

The method of MD simulation of evaporation into the virtual vacuum has been extended to the cases of polyatomic molecules [17], for water and methanol. In the simulations [17], TIP3P model for water [20] and OPLS model for methanol [19] have been used for the intermolecular potentials, in addition to the cut and shifted Coulomb potentials [17].

For polyatomic molecules, the mathematical model of the kinetic boundary condition at the interface is given by [8]

$$f(\boldsymbol{x}, \boldsymbol{\xi}, \eta, t) = \frac{\alpha_e \rho^* + (1-\alpha_c)\rho_w}{[2\pi R T_w(\boldsymbol{x}, t)]^{3/2}} \exp\left\{-\frac{[\xi_i - v_{wi}(\boldsymbol{x}, t)]^2}{2RT_w}\right\} \times \frac{1}{\Gamma(n/2+1)[RT_w(\boldsymbol{x}, t)]^{n/2}} \exp\left[-\frac{\eta^{2/n}}{RT_w(\boldsymbol{x}, t)}\right], \quad (2.88)$$

with Eq. (2.78) for molecules leaving the boundary with the velocity satisfying Eq. (2.77), where $\eta^{2/n}$ ($0 \leqq \eta < \infty$) is the energy of internal motion of one polyatomic molecule with the internal degrees of freedom n,[19] and Γ is the gamma function. The Boltzmann equation and the kinetic boundary condition for polyatomic gas molecules is discussed in Sect. 2.5.1.

As in the case of monatomic molecule [16], the α_e part of the velocity distribution function of polyatomic molecules leaving the interface is found to be the half of the Maxwellian with temperature T_L and zero mean velocity in the case that the liquid temperature is close to the triple point temperature [17]. Again, using Eq. (2.87), the evaporation coefficients for water and methanol are determined. The results are shown in Fig. 2.11. It may be worth noting that the temperature dependence of evaporation coefficients of polyatomic molecules is very similar to that of the monatomic molecule.

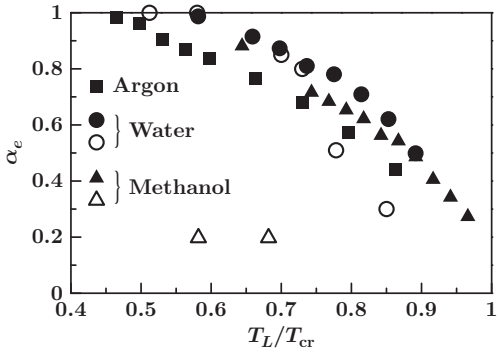

Fig. 2.11 Evaporation coefficients of argon, water, and methanol. The *closed squares* are from Ref. [16], the *closed circles* and *solid triangles* are from Ref. [17], the *open circles* are from Ref. [27], and the *open triangles* are from Ref. [25]. The abscissa of the figure is the liquid temperature T_L divided by the critical temperature T_{cr}, where T_{cr} for argon, TIP3P model for water [20], and OPLS model for methanol [19] are 151, 516, and 404 K, respectively

[19] The internal motions of a polyatomic molecule are the rotational and vibrational motions. Although the rotational motions are usually active at room temperature, the vibrational modes are activated at higher temperature. However, since n is constant in Eq. (2.88), the gas flows associated with the activation and deactivation of the vibrational modes cannot be treated by Eq. (2.88). The distribution of the energy of internal motion is discussed in Sect. 3.1.2.

2.4.3 Condensation Coefficient and KBC in Weak Condensation States

In Sect. 2.4.2, we have constructed the velocity distribution function of molecules evaporating from the interface into the virtual vacuum, and confirmed that the α_e parts of Eqs. (2.81) and (2.88) are precisely reproduced by the MD simulation for the case that the temperature of the liquid phase is low so that the vapor can be regarded as an ideal gas. Next, we construct the complete functional form of Eq. (2.81) by the nonequilibrium MD simulation of various steady condensation states of monatomic molecules [18].

The steady condensation states are realized in the MD simulation by controlling the velocity distribution of molecules impinging on the interface as

$$f = \frac{\rho_{\mathrm{col}}}{(2\pi RT_{\mathrm{col}})^{3/2}} \exp\left(-\frac{\xi_i^2}{2RT_{\mathrm{col}}}\right), \quad \rho_{\mathrm{col}} = \beta\rho^*, \quad T_{\mathrm{col}} = \gamma T_L, \tag{2.89}$$

where we studied 16 cases of $\beta = 1, 2, 3, 4$ and $\gamma = 1, 2, 3, 4$ [18]. Note that ρ^* is the saturated vapor density at the temperature T_L, and the case of $\beta = \gamma = 1$ corresponds to the equilibrium state. The profiles of averaged density for $(\beta, \gamma) = (1, 1)$, $(2, 2)$, and $(4, 4)$ are shown in Fig. 1.1 in Chap. 1, where the parameters (a, b) are used in place of (β, γ).

The condensation at the interface means the transport of mass and energy across the interface, and hence the liquid temperature inevitably increases unless some amount of heat is absorbed appropriately inside the liquid phase. In the MD simulations in Ref. [18], we have fixed the temperature of bulk liquid phase T_L by the velocity control method. This renders the temperature distribution in the bulk liquid phase spatially uniform in spite of the existence of heat flux. We therefore consider that our results are valid in the case that the condensation is weak and hence the temperature gradient in the bulk liquid is negligibly small.

Figure 2.12 shows the velocity distribution of molecules leaving the interface at several pairs of (β, γ), where the velocity distribution function is evaluated on the coordinate that moves with the interface. As clearly shown in the figure, the distribution functions of velocity component normal to the interface are almost the half of the one-dimensional Maxwellian with temperature T_L and zero mean velocity [Fig. 2.12b–d]. On the other hand, the distribution functions of velocity component tangential to the interface deviate from the Maxwellian with temperature T_L as the values of the pair (β, γ) increase [Fig. 2.12e–h]. The results shown in Fig. 2.12 can be formulated into the kinetic boundary condition of the form

$$\begin{aligned} f = {} & [\alpha_e\rho^* + (1-\alpha_c)\rho_w]\frac{1}{\sqrt{2\pi RT_L}} \exp\left(-\frac{\xi_x^2}{2RT_L}\right) \\ & \times \frac{1}{\sqrt{2\pi RT_T}} \exp\left(-\frac{\xi_y^2}{2RT_T}\right) \frac{1}{\sqrt{2\pi RT_T}} \exp\left(-\frac{\xi_z^2}{2RT_T}\right), \end{aligned} \tag{2.90}$$

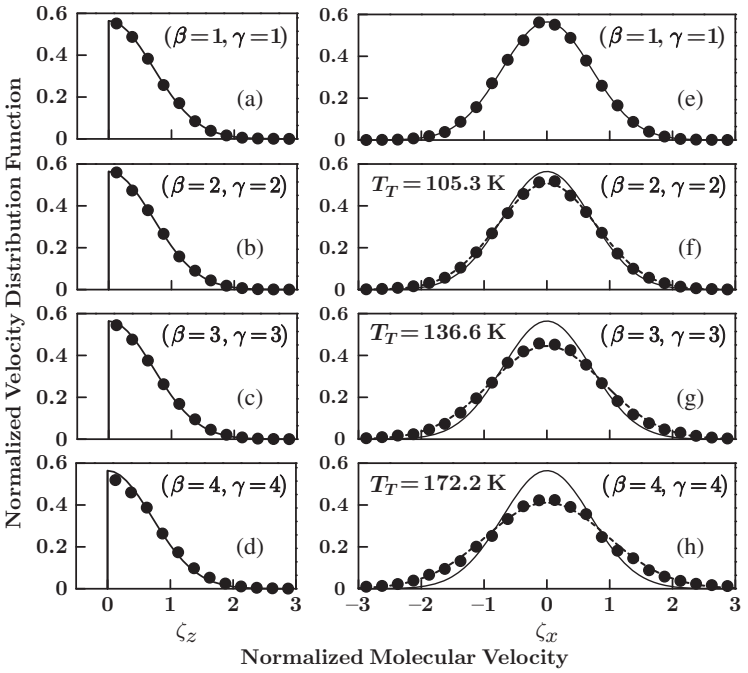

Fig. 2.12 Velocity distribution functions of molecules leaving the interface at several condensation states [18]. The temperature of the bulk liquid is fixed at $T_L = 85$ K by the velocity control method. The equilibrium state at $T_L = 85$ K and at rest is shown in the panels (**a**) and (**e**)

for the molecules leaving the interface with $\xi_x > 0$, where T_T is the temperature associated with the velocity component tangential to the interface, as shown in Fig. 2.12f–h. In Ref. [18], we have shown that T_T has a strong correlation with the energy flux across the interface, although a precise functional relation between T_T and the energy flux still remains unresolved. Nevertheless, we can conclude that Eq. (2.81) can be retrieved for small (β, γ), i.e., in the weak condensation states.

Since we have obtained Eq. (2.90), we can determine the values of condensation coefficient α_c at various nonequilibrium states. To do so, we rewrite the mass flux equation given by Eq. (2.82) as

$$\langle \mathcal{M} \rangle = (\alpha_e \rho^* - \alpha_c \rho_w) \left(\frac{RT_L}{2\pi} \right)^{1/2}, \tag{2.91}$$

by using Eq. (2.90), where the angle brackets indicate the time average. Substituting the evaporation coefficient α_e obtained in Sect. 2.4.1, ρ^*, ρ_w given by Eq. (2.78), and the mass flux $\langle \mathcal{M} \rangle$ obtained by the present MD simulations, we can evaluate the condensation coefficient α_c from Eq. (2.91), and the results are plotted in Fig. 2.13. The figure clearly shows that α_c is almost equal to $\alpha_e = 0.868$ at $T_L = 85$ K [18]. We emphasize that if α_c is a constant, it must be equal to α_e, because f given by Eq. (2.90) should be equal to the Maxwellian with $T_L = T_T$ and $\rho_w = \rho^*$ at the equilibrium state.

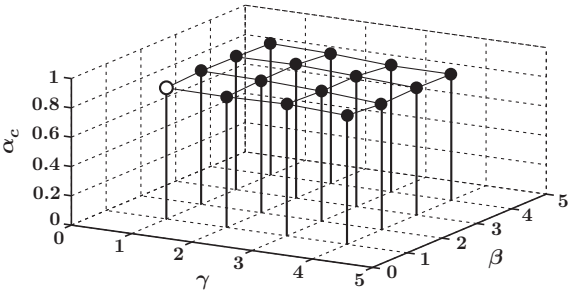

Fig. 2.13 The condensation coefficient at several condensation states [18]. The *open circle* corresponds to the equilibrium state at temperature T_L and at rest

2.5 Asymptotic Analysis of Weak Condensation State of Methanol

In the preceding sections in this chapter, we have demonstrated that the relations connecting the liquid phase, the interface, and the vapor phase can be simplified and reformulated into the KBC at the interface, namely, Eq. (2.81) with Eqs. (2.77) and (2.78) for monatomic molecules and Eq. (2.88) with Eqs. (2.77) and (2.78) for polyatomic molecules. The prerequisites are that (i) the evaporation and condensation should be weak so that the heat flux may be small and the temperature in the liquid near the interface may be regarded as uniform, and that (ii) the temperature of the liquid is not high so that the density of the vapor near the interface may be sufficiently low. The second prerequisite is easily satisfied if the vapor near the interface can be approximated by an ideal gas, and this holds usually. Therefore, we concentrate on the first prerequisite, which can be satisfied if the mass flux across the interface induced by evaporation or condensation is not large.

Since the KBC at the interface is specified, what we should do next is to solve the boundary-value problem of the Boltzmann equation, thereby deriving the boundary conditions for vapor flow in the fluid-dynamics region governed by the set of Navier–Stokes equations or the set of Euler equations. The method of the derivation of the boundary condition for the gas flow in the fluid-dynamics region was devised by Sone [34, 35] on the basis of the kinetic theory of gases. The steady (time-independent) problems associated with monatomic molecules have been solved thoroughly and completely by Sone and his colleagues (see, for example, Refs. [4, 33, 36], and references in his books [34, 35]), including the case of a mixture of a vapor and a noncondensable gas [37, 39].[20] In the following, we apply Sone's asymptotic theory to the case of polyatomic vapor [43].

[20] In Ref. [39], the ghost effect [35] induced by the noncondensable gas is found. The ghost effect has first been found in Ref. [38], and means a finite effect produced by an infinitesimal quantity. For example, in Ref. [38], Sone et al. discussed the temperature field in the limit $\mathrm{Kn} \to 0$ affected by the thermal creep flow that has already vanished in the limit $\mathrm{Kn} \to 0$.

2.5.1 Problem and Formulation

In the presence of evaporation or condensation at the vapor–liquid interface, the vapor near the interface cannot be in an equilibrium state. The typical length scale characterizing the nonequilibrium behavior of the vapor near the interface is the mean free path of the vapor molecules, ℓ. On the other hand, the characteristic length scale of variations in macroscopic variables in the fluid-dynamics region is in general different from ℓ, and let it be L, which is determined by a macroscopic characteristics of vapor flow, such as a linear dimension of a body in the flow. Then, the problem considered here is the case that the Knudsen number defined by

$$\mathrm{Kn} = \frac{\ell}{L}, \tag{2.92}$$

is sufficiently small compared with unity. The nonequilibrium region near the interface is called the Knudsen layer [35]. As we will see later, under the condition that $\mathrm{Kn} \ll 1$, the vapor outside the Knudsen layer is in a local equilibrium state in the leading order of approximation, and hence the vapor flow can be determined by the macroscopic quantities. The appropriate equations governing the macroscopic quantities (the set of Navier–Stokes equations or the set of Euler equations[21]) are derived by applying the asymptotic theory for small Knudsen numbers [35].

The boundary conditions associated with the derived equations for the macroscopic quantities should also be derived from the asymptotic theory [35]. To do so, we have to solve the Boltzmann equation with the kinetic boundary condition at the vapor–liquid interface and the boundary condition at a distant region where the vapor is in a local equilibrium state. This is called the Knudsen layer analysis or the half-space problem of gas flow with evaporation or condensation [35], and extensively studied by Sone and his colleagues for the cases of monatomic molecules [4, 33–37, 39]. The Knudsen layer analysis will be explained in Sect. 2.5.3.

In this subsection, we employ the Boltzmann equation of the Gaussian–BGK model[22] for polyatomic molecules [2]

$$\frac{\partial f}{\partial t} + \xi_j \frac{\partial f}{\partial X_j} = \frac{p}{\mu(1 - \nu + \theta\nu)} \left[G(f) - f \right], \tag{2.93}$$

where $f(\boldsymbol{X}, \boldsymbol{\xi}, \eta, t)$ is the distribution function of molecular velocity and internal motion for polyatomic vapor molecules, t is the time, X_j is the jth component of

[21] Actually, the equations governing the macroscopic quantities outside the Knudsen layer are not always equal to the set of Navier–Stokes equations and the set of Euler equations. Depending upon the macroscopic situation of the flow considered, the derived equations can contain some terms that are not included in the set of Navier–Stokes equations, and hence these equations are sometimes called the fluid-dynamics-type equations [35].

[22] In Ref. [2], the Gaussian–BGK models for both cases of monatomic and polyatomic molecules are discussed. The Boltzmann H-theorem is proved for both cases.

the position vector $\boldsymbol{X}$, ξ_j is the jth component of the molecular velocity vector $\boldsymbol{\xi}$, p is the pressure, μ is the viscosity, and θ and ν are nondimensional parameters ($0 < \theta \leqq 1$ and $-\frac{1}{2} \leqq \nu < 1$).

The symbol G in the right-hand side of Eq. (2.93) represents a nonlinear functional of f given by

$$G(f) = \frac{\rho}{\sqrt{(2\pi)^3 \det(\tau_{ij})}} \exp\left[-\frac{1}{2}(\xi_i - v_i)\tau_{ij}^{-1}(\xi_j - v_j)\right] \times \frac{1}{\Gamma(n/2+1)(RT_{\mathrm{rel}})^{n/2}} \exp\left(-\frac{\eta^{2/n}}{RT_{\mathrm{rel}}}\right), \quad (2.94)$$

where $\eta^{2/n}$ denotes the internal energy of one polyatomic molecule associated with the internal degrees of freedom n, T_{rel} is a relaxation temperature defined in Eq. (2.98), τ_{ij} is a rectified stress tensor defined by Eq. (2.99), Γ is the gamma function, and $\det(\tau_{ij})$ is the determinant of matrix τ_{ij}. The ratio of specific heats of polyatomic molecules γ is related to the parameter n by

$$\gamma = \frac{n+5}{n+3}. \quad (2.95)$$

The most important feature of the Gaussian–BGK Boltzmann equation (2.93) and (2.94) is that the mathematical proof of the Boltzmann H-theorem[23] has been given for the parameters θ and ν in the range $0 < \theta \leqq 1$ and $-\frac{1}{2} \leqq \nu < 1$ [2]. The H-theorem has not been proved for other models of Boltzmann equations for polyatomic molecules.

The macroscopic variables are defined by the four-fold integrals of f with respect to $\boldsymbol{\xi}$ and η as follows:

$$\rho = \int f \, \mathrm{d}\boldsymbol{\xi} \, \mathrm{d}\eta, \quad \rho v_i = \int \xi_i f \, \mathrm{d}\boldsymbol{\xi} \, \mathrm{d}\eta, \quad 3\rho R T_{\mathrm{tr}} = \int (\xi_j - v_j)^2 f \, \mathrm{d}\boldsymbol{\xi} \, \mathrm{d}\eta, \quad (2.96)$$

$$n\rho T_{\mathrm{int}} = 2\int \eta^{2/n} f \, \mathrm{d}\boldsymbol{\xi} \, \mathrm{d}\eta, \quad \rho\Theta_{ij} = \int (\xi_i - v_i)(\xi_j - v_j) f \, \mathrm{d}\boldsymbol{\xi} \, \mathrm{d}\eta, \quad (2.97)$$

$$(3+n)T = 3T_{\mathrm{tr}} + nT_{\mathrm{int}}, \quad p = \rho R T, \quad T_{\mathrm{rel}} = \theta T + (1-\theta)T_{\mathrm{int}}, \quad (2.98)$$

$$\rho\tau_{ij} = \theta p \delta_{ij} + (1-\theta)[(1-\nu)\rho R T_{\mathrm{tr}}\delta_{ij} + \nu\rho\Theta_{ij}], \quad (2.99)$$

where ρ is the density, v_i is the vapor velocity, T is the temperature, T_{tr} and T_{int} are, respectively, the temperatures associated with the translational and internal motions of the molecule, δ_{ij} is the Kronecker delta, and $\rho\Theta_{ij}$ is the stress tensor. The four-fold integration with respect to $\boldsymbol{\xi}$ and η is carried out over the whole space of $\boldsymbol{\xi}$ and $0 \leqq \eta < \infty$. The parameters θ, ν, and n are chosen so that the Prandtl number

[23] See Footnote 16.

and viscosity coefficients in the Gaussian–BGK model can be adapted for given (or experimental) values by the relation

$$\frac{2}{3} \leqq \mathrm{Pr} = \frac{1}{1-\nu+\theta\nu} < \infty, \tag{2.100}$$

$$0 \leqq \frac{\mu_b}{\mu} = \frac{2n}{3+n}\frac{1-\nu+\theta\nu}{3\theta} \leqq \frac{n}{(3+n)\theta}, \tag{2.101}$$

for $0 < \theta \leqq 1$ and $-\frac{1}{2} \leqq \nu < 1$, where Pr $(= c_p\mu/\kappa)$ is the Prandtl number and μ_b is the bulk viscosity (c_p is the specific heat at constant pressure and κ is the thermal conductivity coefficient). The case that $\theta = 1$ and $\nu = n = 0$ corresponds to the BKW equation for monatomic molecules introduced in Sect. 2.3.1, and methanol at room temperature may be modeled by $(\theta, \nu, n) = (0.6471, -0.5, 6)$. The mean free path ℓ of the Gaussian–BGK model is given by

$$\ell = (1-\nu+\theta\nu)\frac{\mu}{p}\frac{2\sqrt{2RT}}{\sqrt{\pi}}. \tag{2.102}$$

where $p/[\mu(1-\nu+\theta\nu)]$ is the mean collision frequency.

As mentioned in Footnote 19 in this chapter, since the parameter n is a constant in the Gaussian–BGK model (2.93), (2.94), (2.95), (2.96), (2.97), (2.98), and (2.99), the activation and deactivation of vibrational modes of molecular internal motions cannot be described by Eqs. (2.93), (2.94), (2.95), (2.96), (2.97), (2.98), and (2.99). For the temperature range treated in this book, the molecular internal motions are the rotational motions.

The boundary condition for the Gaussian–BGK Boltzmann equation (2.93) and (2.94) is given by [see Eq. (2.88)]

$$\begin{aligned} f(\boldsymbol{X}, \boldsymbol{\xi}, \eta, t) = {} & \frac{\alpha_e\rho^* + (1-\alpha_c)\rho_w}{[2\pi RT_w(\boldsymbol{X}, t)]^{3/2}} \exp\left\{-\frac{[\xi_i - v_{wi}(\boldsymbol{X}, t)]^2}{2RT_w(\boldsymbol{X}, t)}\right\} \\ & \times \frac{1}{\Gamma(n/2+1)[RT_w(\boldsymbol{X}, t)]^{n/2}} \exp\left[-\frac{\eta^{2/n}}{RT_w(\boldsymbol{X}, t)}\right], \end{aligned} \tag{2.103}$$

and

$$\begin{aligned} \rho_w = {} & -\left[\frac{2\pi}{RT_w(\boldsymbol{X}, t)}\right]^{1/2} \\ & \times \int_{\substack{0 \leqq \eta < \infty \\ \xi_j n_j(\boldsymbol{X}, t) < v_{wj}(\boldsymbol{X}, t) n_j(\boldsymbol{X}, t)}} \left[\xi_j - v_{wj}(\boldsymbol{X}, t)\right] n_j(\boldsymbol{X}, t) f(\boldsymbol{X}, \boldsymbol{\xi}, \eta, t)\, \mathrm{d}\boldsymbol{\xi}\, \mathrm{d}\eta, \end{aligned} \tag{2.104}$$

for molecules leaving the boundary with the velocity satisfying

$$\boldsymbol{\xi} \cdot \boldsymbol{n}(\boldsymbol{X}, t) > \boldsymbol{v}_w(\boldsymbol{X}, t) \cdot \boldsymbol{n}(\boldsymbol{X}, t), \tag{2.105}$$

at a point $\boldsymbol{X}$ on the interface and at a time t, where $T_w(\boldsymbol{X}, t)$ and $\boldsymbol{v}_w(\boldsymbol{X}, t)$ are the temperature and velocity at the interface, $\boldsymbol{n}(\boldsymbol{X}, t)$ is the unit vector normal to the interface and pointing to the vapor phase. Equation (2.103) is an extension of the mixed-type boundary condition (2.81) to polyatomic molecules, and its functional form with respect to $\boldsymbol{\xi}$ and η is equal to the half of the equilibrium distribution function of polyatomic molecules with the ratio of specific heats $\gamma = (n+5)/(n+3)$ at the equilibrium state with the temperature T_w and the mean velocity $\boldsymbol{v}_w$.

The condition of a weak nonequilibrium state can be expressed as

$$\left| \frac{\boldsymbol{v}}{\sqrt{2RT_0}} \right| \ll 1, \quad \left| \frac{p - p_0}{p_0} \right| \ll 1, \quad \left| \frac{T - T_0}{T_0} \right| \ll 1, \tag{2.106}$$

where p_0 and T_0 are the pressure and temperature in a reference equilibrium state at rest. Equation (2.106) should be viewed as a sufficient condition for the weak evaporation/condensation state where the mass flux across the interface is so small that the liquid phase may be regarded as in a local equilibrium state and the boundary condition (2.103) may hold. In the asymptotic analysis for small Knudsen numbers, we have to specify how the quantities in Eq. (2.106) are small compared with the small Knudsen number Kn (see Sect. 2.5.2).

2.5.2 Asymptotic Analysis for Small Knudsen Numbers

We study the time-independent solution for the boundary-value problem (2.93), (2.94), (2.95), (2.96), (2.97), (2.98), and (2.99) with (2.103), assuming that the condensation is weak in the sense of Eq. (2.106), and the Knudsen number defined by Eqs. (2.92) and (2.102) is sufficiently small compared with unity.

According to Refs. [34, 35], we seek a moderately varying solution of Gaussian–BGK model for polyatomic gas in a power series for small Kn (S expansion [35]),

$$\phi = k\phi_{S1} + k^2\phi_{S2} + \cdots, \quad k = \frac{\sqrt{\pi}}{2}\mathrm{Kn} \ll 1, \tag{2.107}$$

where $\phi = (f - f_0)/f_0$ is a nondimensional distribution function, f_0 is an equilibrium distribution in a reference equilibrium state at rest, and Kn is the Knudsen number defined by Eqs. (2.92) and (2.102) at the reference state. The mean free path ℓ_0 is given by

$$\ell_0 = (1 - \nu + \theta\nu)\,\frac{\mu_0}{p_0}\,\frac{2\sqrt{2RT_0}}{\sqrt{\pi}}, \tag{2.108}$$

(μ_0 is the viscosity in the reference state). The moderately varying solution is often called the fluid-dynamics part of the solution of the problem [35]. The application of the S expansion (2.107) means that we consider the situation where

$$\left|\frac{\boldsymbol{v}}{\sqrt{2RT_0}}\right| = O(k), \quad \left|\frac{p-p_0}{p_0}\right| = O(k), \quad \left|\frac{T-T_0}{T_0}\right| = O(k). \tag{2.109}$$

In general, the Boltzmann equation (2.60) can be nondimensionalized as, for the time-independent problems,

$$\zeta_j \frac{\partial \phi}{\partial x_j} = \frac{1}{k}\hat{J}(\phi), \tag{2.110}$$

where $\zeta_j = \xi_j/\sqrt{2RT_0}$ is the nondimensional molecular velocity, $x_j = X_j/L$ is the nondimensionalized spatial coordinate, and $k^{-1}\hat{J}(\phi)$ is the nondimensionalized collision term of Eq. (2.60). The Gaussian–BGK Boltzmann equation can also be expressed as Eq. (2.110). From Eq. (2.110), one can immediately see that $\hat{J}(\phi) = 0$ in the leading order of approximation, if the moderately varying solution ϕ and its derivative with respect to x_j are of the order of k. That is, the moderately varying solution is a local equilibrium distribution function in the leading order of approximation, because the collision term of the Boltzmann equation vanishes when and only when the distribution function is an equilibrium or a local equilibrium distribution function. The moderately varying solution is, therefore, characterized by the macroscopic variables, i.e., the velocity, the density, and the temperature. In the following, we will derive the equations governing these macroscopic variables and the boundary conditions for the equations.

Substituting the power series (2.107) into the Boltzmann equation (2.110), and equating the coefficients of the same powers of k, we have a series of equations

$$\hat{L}(\phi_{S1}) = 0, \tag{2.111}$$

$$\hat{L}(\phi_{S2}) = \hat{N}(\phi_{S1}) + \zeta_j \frac{\partial \phi_{S1}}{\partial x_j}, \tag{2.112}$$

$$\cdots\cdots$$

where $\hat{L}$ is a linearized integral operator and $\hat{N}$ is a nonlinear integral operator, both of which are derived from the nondimensional collision term $\hat{J}$ in Eq. (2.110), and their explicit forms depend on the collision term. The homogeneous linear integral equation for ϕ_{S1}, Eq. (2.111), has nontrivial solutions corresponding to a local equilibrium solution, and hence the inhomogeneous term of Eq. (2.112) has to satisfy adequate solvability conditions in order that ϕ_{S2} is determinable. In addition to the fact that the solvability conditions render the asymptotic expansion (2.107) uniformly valid in the region of $x_i = O(1)$, the solvability conditions themselves are the equations governing the macroscopic variables in the region of $x_i = O(1)$, i.e., in the fluid-dynamics region [35].

For the Gaussian–BGK Boltzmann equation, the procedures to derive the equations governing the macroscopic variables are summarized in Ref. [43] for the time-independent problem and in Ref. [14] for the time-dependent (linear) problem. The results for the time-independent problem are summarized as

$$\frac{\partial P_{S1}}{\partial x_i} = 0, \tag{2.113}$$

$$\frac{\partial u_{iS1}}{\partial x_i} = 0, \tag{2.114}$$

$$u_{jS1}\frac{\partial u_{iS1}}{\partial x_j} = -\frac{1}{2}\frac{\partial P_{S2}}{\partial x_i} + \frac{\Pr}{2}\frac{\partial^2 u_{iS1}}{\partial x_j^2}, \tag{2.115}$$

$$u_{jS1}\frac{\partial \tau_{S1}}{\partial x_j} = \frac{1}{2}\frac{\partial^2 \tau_{S1}}{\partial x_j^2}, \tag{2.116}$$

$$\frac{\partial u_{iS2}}{\partial x_i} + u_{iS1}\frac{\partial \omega_{S1}}{\partial x_i} = 0, \tag{2.117}$$

$$u_{jS1}\frac{\partial u_{iS2}}{\partial x_j} + (u_{jS2} + \omega_{S1}u_{jS1})\frac{\partial u_{iS1}}{\partial x_j} = -\frac{1}{2}\frac{\partial}{\partial x_i}\left(P_{S3} + \frac{\Pr}{2}\frac{\partial^2 \tau_{S1}}{\partial x_j^2}\right) + \frac{\Pr}{2}\frac{\partial^2 u_{iS2}}{\partial x_j^2} + \frac{\Pr}{2}\frac{\partial}{\partial x_i}\left[\beta\tau_{S1}\left(\frac{\partial u_{iS1}}{\partial x_j} + \frac{\partial u_{jS1}}{\partial x_i}\right)\right], \tag{2.118}$$

$$u_{jS1}\frac{\partial \tau_{S2}}{\partial x_j} + (u_{jS2} + \omega_{S1}u_{jS1})\frac{\partial \tau_{S1}}{\partial x_j} - \frac{2}{5+n}u_{jS1}\frac{\partial P_{S2}}{\partial x_j} = \frac{\Pr}{5+n}\left(\frac{\partial u_{iS1}}{\partial x_j} + \frac{\partial u_{jS1}}{\partial x_i}\right)^2 + \frac{1}{2}\frac{\partial^2}{\partial x_j^2}\left(\tau_{S2} + \frac{\beta}{2}\tau_{S1}^2\right), \tag{2.119}$$

where the macroscopic variables ω_{Sm}, u_{iSm}, τ_{Sm}, and P_{Sm} ($m = 1, 2, 3$) are the expansion coefficients of nondimensional density $\omega = (\rho - \rho_0)/\rho_0$, nondimensional velocity $u_i = v_i/\sqrt{2RT_0}$, nondimensional temperature $\tau = (T - T_0)/T_0$, and nondimensional pressure $P = (1 + \omega)(1 + \tau)$, respectively, and the nondimensional parameter β in Eqs. (2.118) and (2.119) comes from the assumption that $\mu = \mu_0(1 + \tau)^\beta$.

We shall remark that (i) Eqs. (2.113), (2.114), (2.115), (2.116), (2.117), (2.118), and (2.119) are the same as those derived from the asymptotic analysis of the BKW equation [35], if $n = 0$, $\Pr = 1$, and $\beta = 1$; (ii) the temperature associated with the molecular translational motion T_{tr} and that with the molecular internal motion T_{int} are equal to the vapor temperature T up to the order shown above; (iii) the bulk

viscosity does not appear up to the order shown above, while it appears in the third order in the time-dependent problem [14].

From Eq. (2.113), the vapor pressure is spatially uniform in the leading order of approximation. Equation (2.114) is the solenoidal condition for the vapor velocity in the leading order. However, the vapor flow is a compressible flow. In fact, the incompressibility condition

$$u_{iS1}\frac{\partial \omega_{S1}}{\partial x_i} = 0, \tag{2.120}$$

does not hold due to Eq. (2.117), and the energy equation (2.116) is different from that of incompressible flows in fluid dynamics,

$$\frac{n+3}{n+5}u_{iS1}\frac{\partial \tau_{S1}}{\partial x_j} = \frac{1}{2}\frac{\partial^2 \tau_{S1}}{\partial x_j^2}. \tag{2.121}$$

2.5.3 Boundary Condition for the Equations in Fluid-Dynamics Region

The final topic of this chapter is the derivation of the boundary conditions for the macroscopic equations (2.113), (2.114), (2.115), and (2.116). Thereby, the microscopic information connecting the liquid phase and the vapor phase through the interface can be transformed into the relations in terms of macroscopic variables. The microscopic information is included in the macroscopic relations as numerical constants, called the slip coefficients [35].

The boundary conditions for the macroscopic equations and the slip coefficients are derived by solving the Boltzmann equation in the Knudsen layer with the kinetic boundary condition (2.103), (2.104), and (2.105), and the procedure is called the Knudsen layer analysis [35]. Since the characteristic length scale in the Knudsen layer is the mean free path of the vapor molecules, we introduce a stretched independent variable y normal to the interface,

$$y = \frac{(x_i - x_{wi})n_i}{k}, \tag{2.122}$$

where x_{wi} represents the coordinate of the point on the interface. The Boltzmann equation (2.110) can be expressed as[24]

[24] Sects. 2.5.2 and 2.5.3 are concerned with the time-independent problem. However, even in a time-dependent problem, if the characteristic time scale t_0 of the problem is large so that $\ell_0/t_0\sqrt{2RT_0} = O(k)$, then the time derivative term in the Boltzmann equation drops in the Knudsen layer in the leading order of approximation, and hence the vapor flow in the Knudsen layer can be treated as a time-independent flow in the leading order of approximation, where the time variable t is included as a parameter.

$$\zeta_i n_i \frac{\partial \phi_{K1}}{\partial y} = \hat{L}(\phi_{K1}), \tag{2.123}$$

in the leading order of approximation, where the nondimensional distribution function ϕ is decomposed into the sum of the fluid-dynamics part ϕ_S and the Knudsen layer correction ϕ_K, and ϕ_K is expanded as

$$\phi_K = k\phi_{K1} + k^2\phi_{K2} + \cdots . \tag{2.124}$$

Furthermore, it is assumed that ϕ_K decays faster than any inverse power of y [35]. Since the coordinate y is stretched, the fluid-dynamics region is located at $y \to \infty$. The Knudsen layer analysis is therefore equivalent to the so-called half-space problem of the Boltzmann equation [35].

The important point is that the solution of the half-space problem of the Boltzmann equation exists only when the condition at infinity satisfies some relations [35]. Therefore, at the same time when we obtain the solution of the half-space problem or the solution in the Knudsen layer (Knudsen layer function), the condition for the macroscopic variables in the fluid-dynamics region (condition at infinity for the half-space problem) are also obtained, and the microscopic information is incorporated into the condition for the macroscopic variables. This is the boundary condition for the macroscopic equations in the fluid-dynamics region.

If the kinetic boundary condition at the interface has a Maxwellian-like functional form with respect to $\boldsymbol{\xi}$, the solution of the half-space problem can be described with some universal functions independent of the multiplication factor of the Maxwellian-like function [42]. In Ref. [42], although the proof has been given for the Boltzmann equation of monatomic molecules, its extension to the Gaussian–BGK Boltzmann equation is straightforward.

For the Gaussian–BGK Boltzmann equation, the Knudsen layer analysis can be carried out in the same way as those for the BKW equation in Refs. [33, 36] (see also [35]), and thereby the Knudsen layer corrections and the boundary condition for the macroscopic equations with slip coefficients can be obtained. The results in the leading order of approximation are as follows:

$$(u_{iS1} - u_{wi1})t_i = 0, \tag{2.125}$$

$$u_{iK1} = 0, \tag{2.126}$$

$$P_{S1} - P_{w1} = \frac{\alpha_e}{\alpha_c}\left(C_4^* - 2\sqrt{\pi}\frac{1-\alpha_c}{\alpha_c}\right)u_{iS1}n_i + \frac{\alpha_e - \alpha_c}{\alpha_c}, \tag{2.127}$$

$$\tau_{S1} - \tau_{w1} = d_4^* u_{iS1} n_i, \tag{2.128}$$

$$\omega_{K1} = u_{iS1} n_i \Omega_4^*(y), \tag{2.129}$$

$$\tau_{\mathrm{tr}K1} = u_{iS1} n_i \Theta_{4\mathrm{tr}}^*(y), \tag{2.130}$$

$$\tau_{\mathrm{int}K1} = u_{iS1} n_i \Theta_{4\mathrm{int}}^*(y). \tag{2.131}$$

Here, (i) the fluid-dynamics parts, u_{iS1}, τ_{S1}, and P_{S1}, are evaluated on the interface,[25] and they are independent of y. (ii) u_{wi1}, τ_{w1}, and P_{w1} are, respectively, the first expansion coefficients of the nondimensional velocity, temperature of the interface, and the saturated vapor pressure at the temperature T_w, e.g., $v_{wi}/\sqrt{2RT_w} = ku_{wi1} + k^2u_{wi2} + \cdots$, and so on. (iii) $u_{wi}n_i$ should vanish in the time-independent boundary-value problem. (iv) u_{iK1}, ω_{K1}, $\tau_{\mathrm{tr}K1}$, and $\tau_{\mathrm{int}K1}$ are, respectively, the Knudsen layer corrections for the velocity, density, and temperature associated with translational and internal motions. (v) n_i and t_i are unit vectors normal and tangential to the interface, respectively. (vi) Equation (2.127) is a generalization of the result from the complete-condensation condition [36] according to Ref. [42].

It is important to note that the condensation coefficient α_c varies according with the flow condition, whereas the evaporation coefficient α_e is constant if T_w is constant. In the limit to the vapor–liquid equilibrium state, the evaporation or condensation ceases, i.e., $u_{iS1}n_i \to 0$ in Eqs. (2.127) and (2.128), and the vapor temperature and pressure should be equal to T_w and p^*, respectively. Accordingly, $\alpha_c \to \alpha_e$ in the limit of $u_{iS1}n_i \to 0$. We therefore require another information that gives α_c as a function of $u_{iS1}n_i$. This is one of main topics of Sect. 3. A theoretical formulation for constructing α_c as a linear function of $u_{iS1}n_i$ is shown in the next subsection.

The values of slip coefficients C_4^* and d_4^* and the functional forms of Knudsen layer functions $\Omega_4^*(y)$, $\Theta_{4\mathrm{tr}}^*(y)$, and $\Theta_{4\mathrm{int}}^*(y)$ are dependent on the parameters θ and ν in the Gaussian–BGK model and the internal degrees of freedom n. In the present study, we set $\theta = 0.6471$, $\nu = -0.5$, $n = 6$, $\mathrm{Pr} = 0.86$, and the ratio of specific heats 1.22 corresponding to methanol vapor at room temperature. In the case, we obtain [43][26]

$$C_4^* = -2.0723, \quad d_4^* = -0.2185, \tag{2.132}$$

and

$$\Omega_4^*(0) = 0.475, \quad \Theta_{4\mathrm{tr}}^*(0) = -0.083, \quad \Theta_{4\mathrm{int}}^*(0) = 0.145. \tag{2.133}$$

The slip coefficients and the Knudsen layer functions for the BKW model and for the Boltzmann equation for hard-sphere gas are precisely determined and tabulated in the book [35]: for hard-sphere gas,

$$C_4^* = -2.1412, \quad d_4^* = -0.4557, \tag{2.134}$$

$$\Omega_4^*(0) = 0.37815, \quad \Theta_4^*(0) = 0.05206, \tag{2.135}$$

[25] The fluid-dynamics parts are unchanged in the Knudsen layer and the Knudsen-layer corrections rapidly vanish $y \to \infty$. Therefore, u_{iS1}, τ_{S1}, and P_{S1} in Eq. (2.125) and Eqs. (2.127), (2.128), (2.129), (2.130), and (2.131) are, respectively, equal to the velocity, temperature, and pressure of the vapor at the outer edge of the Knudsen layer in the approximation of $O(k)$.

[26] These values have recently been corrected by M. Inaba as follows (private communication): $C_4^* = -2.0719$, $d_4^* = -0.1921$, $\Omega_4^*(0) = 0.5006$, $\Theta_{4tr}^*(0) = -0.1090$, and $\Theta_{4int}^*(0) = 0.1190$.

and for the BKW model,

$$C_4^* = -2.13204, \quad d_4^* = -0.44675, \tag{2.136}$$

$$\Omega_4^*(0) = 0.36303, \quad \Theta_4^*(0) = 0.03717. \tag{2.137}$$

As can be seen from Eqs. (2.132), (2.134), and (2.136), C_4^* for the Gaussian–BGK model for polyatomic molecules is rather close to those for monatomic gas. The coefficient d_4^* for polyatomic molecules is, however, about a half of that for monatomic gas for the present case of $\theta = 0.6471$, $\nu = -0.5$, and $n = 6$.

The dimensional expressions of Eqs. (2.127) and (2.128), extended to time-dependent problems,[27] can be written as

$$\frac{p - p^*}{p^*} = \frac{\alpha_e}{\alpha_c}\left(C_4^* - 2\sqrt{\pi}\frac{1-\alpha_c}{\alpha_c}\right)\frac{[v_i - v_{wi}(\boldsymbol{X}, t)]\, n_i(\boldsymbol{X}, t)}{\sqrt{2RT_w(\boldsymbol{X}, t)}} + \frac{\alpha_e - \alpha_c}{\alpha_c}, \tag{2.138}$$

$$\frac{T - T_w(\boldsymbol{X}, t)}{T_w(\boldsymbol{X}, t)} = d_4^* \frac{[v_i - v_{wi}(\boldsymbol{X}, t)]\, n_i(\boldsymbol{X}, t)}{\sqrt{2RT_w(\boldsymbol{X}, t)}}, \tag{2.139}$$

where the saturated pressure $p^* = \rho^* R T_w$ is a function of $\boldsymbol{X}$ and t through $T_w(\boldsymbol{X}, t)$.

2.5.4 Condensation Coefficient as a Linear Function of Mass Flux

In the weak nonequilibrium problems in the sense of Eq. (2.109), all the perturbations, including the difference between α_c and α_e, are of the order of k. We may therefore assume that[28]

$$\alpha_c = \alpha_e + \Lambda \frac{(v_i - v_{wi})n_i}{\sqrt{2RT_w}}, \tag{2.140}$$

where Λ is independent of $(v_i - v_{wi})n_i$ and may be a function of T_w. The factor Λ contains the microscopic information of interface, which cannot be deduced by the kinetic theory of gases. The determination of the factor Λ may be possible by detailed nonequilibrium MD simulations, although it has not been performed yet. The experimental study presented in Sect. 3 is an only successful achievement for the determination of Λ up to now. By using Eq. (2.140), Eq. (2.138) is transformed as

$$\frac{p}{p^*} = 1 + \left(C_4^* + 2\sqrt{\pi} - \frac{2\sqrt{\pi}}{\alpha_e} - \frac{\Lambda}{\alpha_e}\right)\frac{(v_i - v_{wi})n_i}{\sqrt{2RT_w}}, \tag{2.141}$$

---

[27] See Footnote 24.

[28] The dimensionless mass flux $\rho(v_i - v_{wi})n_i/(\rho^*\sqrt{2RT_w})$ is approximately equal to $(v_i - v_{wi})n_i/\sqrt{2RT_w}$ in the accuracy of $O(k)$ since $(v_i - v_{wi})n_i/\sqrt{2RT_w} = O(k)$ and $\rho/\rho^* = 1 + O(k)$.

in the approximation up to $O(k)$. The boundary conditions for the fluid-dynamics region are Eqs. (2.141) and (2.139).

In Ref. [21], a nondimensional parameter A is defined by

$$A = \frac{\alpha_e \rho^* - \alpha_c \rho_w}{\rho^* - \rho_w}, \tag{2.142}$$

and evaluated as constants, $A = 0.52$ for water and $A = 0.50$ for methanol, from the analysis of a number of data obtained by the shock-tube experiment of weak condensation at room temperature (see Sect. 3).[29] We here derive the relation between the factor Λ in Eq. (2.140) and the parameter A.

In the mass flux equation,

$$\mathcal{M} = (\alpha_e \rho^* - \alpha_c \rho_w)\sqrt{\frac{RT_w}{2\pi}}, \tag{2.143}$$

$\mathcal{M}$ denotes the mass flux across the interface. Since the vapor flow in the Knudsen layer concerned is a time-independent flow, $\mathcal{M}$ can be replaced by $\rho(v_i - v_{wi})n_i$ at the outer edge of the Knudsen layer, and we have

$$\rho(v_i - v_{wi})n_i = (\alpha_e \rho^* - \alpha_c \rho_w)\sqrt{\frac{RT_w}{2\pi}}. \tag{2.144}$$

Dividing Eq. (2.138) by Eq. (2.139) and neglecting the terms of $O(k^2)$ gives

$$\frac{\rho}{\rho^*} = \frac{\alpha_e}{\alpha_c}\left[1 + \left(C_4^* - d_4^* + 2\sqrt{\pi} - \frac{2\sqrt{\pi}}{\alpha_c}\right)\frac{(v_i - v_{wi})n_i}{\sqrt{2RT_w}}\right], \tag{2.145}$$

where α_c has been treated as $O(1)$ and Eq. (2.140) has not been used yet. Substituting $\rho/\rho^* = \alpha_e/\alpha_c$ obtained from Eq. (2.145) into Eq. (2.144) yields

$$\frac{\rho_w}{\rho^*} = \frac{\alpha_e}{\alpha_c}\left[1 - \frac{2\sqrt{\pi}}{\alpha_c}\frac{(v_i - v_{wi})n_i}{\sqrt{2RT_w}}\right], \tag{2.146}$$

in the approximation up to $O(k)$, where we still do not use Eq. (2.140). Substituting Eqs. (2.140) and (2.146) into Eq. (2.142), and taking the limit of $(v_i - v_{wi})n_i \to 0$, we obtain

$$\Lambda = 2\sqrt{\pi}\left(\frac{\alpha_e}{A} - 1\right). \tag{2.147}$$

Using $\alpha_e = 0.86$ for both water and methanol [17], we can determine Λ as follows:

$$\Lambda = 2.3 \text{ for water}, \quad \Lambda = 2.6 \text{ for methanol}. \tag{2.148}$$

[29] Apparently, the right-hand side of Eq. (2.142) is equal to the ratio of the mass flux given by Eq. (2.82) to that in the case of complete-condensation condition given by Eq. (2.80).

2.6 Criticism on Hertz–Knudsen–Langmuir and Schrage Formulas

In Sect. 2.5.3, the boundary conditions for the macroscopic equations in the fluid-dynamics region, Eqs. (2.127) and (2.128), are derived by solving the Boltzmann equation in the Knudsen layer on the interface. Without solving the Boltzmann equation, the boundary conditions can never be obtained. However, several formulas have been proposed without solving the Boltzmann equation, and surprisingly, these formulas are used as the boundary conditions for the macroscopic equations in various applications still now. They are constructed from the mass flux equation (2.82) by replacing the unknown variable ρ_w with some functions of ρ, T, and $(v_i - v_{wi})n_i$ at the outer edge of the Knudsen layer [7]. In the following, we take up typical two formulas and compare them with Eqs. (2.127) and (2.128).

The first one is known as the Hertz–Knudsen–Langmuir formula [7],

$$\mathcal{M}_{HKL} = \frac{1}{\sqrt{2\pi R}} \left(\alpha_e \frac{p^*}{\sqrt{T_w}} - \alpha_c \frac{p}{\sqrt{T}} \right), \tag{2.149}$$

where α_e and α_c are the evaporation and condensation coefficients, for which $\alpha_e = \alpha_c = \alpha$ is sometimes used. The second one is the Schrage formula [7],

$$\mathcal{M}_{Sch} = \frac{2\alpha}{(2-\alpha)\sqrt{2\pi R}} \left(\frac{p^*}{\sqrt{T_w}} - \frac{p}{\sqrt{T}} \right), \tag{2.150}$$

where α is a nondimensional parameter for evaporation and condensation. Both Eqs. (2.149) and (2.150) are produced by replacing ρ_w in Eq. (2.82) by some functions consisted of p, T, and $(v_i - v_{wi})n_i$, although there is no justification for such a replacement without solving the Boltzmann equation.

The inappropriateness of the Schrage formula can easily be demonstrated: In fact, for given T_w and p^*, $\mathcal{M}_{Sch}$ vanishes if a pair (p, T) satisfies the relation

$$\frac{T}{T_w} = \left(\frac{p}{p^*} \right)^2. \tag{2.151}$$

That is, the mass flux across the interface vanishes for an infinite number of pairs (p, T) that satisfy Eq. (2.151) in spite of vapor–liquid nonequilibrium states. This contradicts the fact that the mass flux evaluated from the solution of the Boltzmann equation vanishes only in the vapor–liquid equilibrium state, i.e., $p = p^*$ and $T = T_w$, as shown by Eqs. (2.127) and (2.128). For the Hertz–Knudsen–Langmuir formula, the same discussion can be applied for pairs (p, T) satisfying

$$\frac{T}{T_w} = \left(\frac{\alpha_c p}{\alpha_e p^*} \right)^2, \tag{2.152}$$

instead of Eq. (2.151).

Furthermore, we express a pair (p, T) satisfying Eq. (2.151) or (2.152) as $(p^\dagger, T^\dagger)$, and consider the linearization around $(p^\dagger, T^\dagger)$. Substituting $p = p^\dagger \times (1 + P^\dagger)$ and $T = T^\dagger(1 + \tau^\dagger)$ into Eqs. (2.149) and (2.150), and linearizing the resulting equations under the assumption of $|P^\dagger| \ll 1$ and $|\tau^\dagger| \ll 1$, we have

$$\mathcal{M}_{HKL} = \frac{\alpha_e p^*}{\sqrt{2\pi RT_w}} \left(\frac{1}{2}\tau^\dagger - P^\dagger \right), \tag{2.153}$$

$$\mathcal{M}_{Sch} = \frac{2\alpha}{2-\alpha} \frac{p^*}{\sqrt{2\pi RT_w}} \left(\frac{1}{2}\tau^\dagger - P^\dagger \right). \tag{2.154}$$

That is, the both formulas predict that the evaporation ($\mathcal{M} > 0$) occurs when $\tau^\dagger > 2P^\dagger$ even if $T - T_w > 0$, and the condensation ($\mathcal{M} < 0$) occurs when $\tau^\dagger < 2P^\dagger$ even if $p - p^* < 0$. However, as can be seen from Eqs. (2.127) and (2.128) and from Fig. 2.14, the evaporation ($u_{iS1}n_i > 0$) occurs only when $T - T_w < 0$ and the condensation ($u_{iS1}n_i < 0$) occurs only when $p - p^* > 0$ (if $\alpha_e = \alpha_c = 1$). Although Eqs. (2.127) and (2.128) are results in the leading order of approximation for $u_{iS1}n_i = O(k)$, according to the numerical solution for nonlinear problems [35, 42], it is confirmed that the steady evaporation occurs only when $T - T_w < 0$ and the steady condensation occurs only when $p - p^* > 0$. Thus, the both formulas are wrong and of no use.

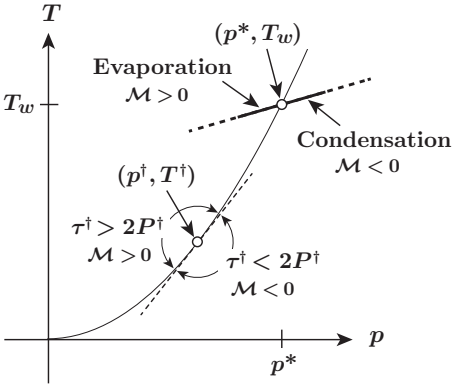

Fig. 2.14 The boundary conditions for macroscopic equations, Eqs. (2.127) and (2.128), are shown by a *bold straight line* passing through the vapor–liquid equilibrium point (p^*, T_w) in the (p, T) plane. The parabola in the figure means Eqs. (2.151) or (2.152). The Hertz–Knudsen–Langmuir and Schrage formulas divide the neighborhood of a zero-mass-flux point $(p^\dagger, T^\dagger)$ on the parabola into the evaporation and condensation regions with a *thin dashed line* $\tau^\dagger = 2P^\dagger$

References

1. M.P. Allen, D.J. Tildesley, *Computer Simulation of Liquids* (Clarendon Press, Oxford, 1987)
2. P. Andries, P.L. Tallec, J.P. Perlat, B. Perthame, Gaussian – BGK model of Boltzmann equation with small Prandtl number. Eur. J. Mech. B-Fluids **19**, 813–830 (2000)

3. S.I. Anisimov, D.O. Dunikov, S.P. Malyshenko, V.V. Zhakhovskii, Properties of a liquid – gas interface at high-rate evaporation. J. Chem. Phys. **110**, 8722–8729 (1999)
4. K. Aoki, K. Nishino, Y. Sone, H. Sugimoto, Numerical analysis of steady flows of a gas condensing on or evaporating from its plane condensed phase on the basis of kinetic theory: Effect of gas motion along the condensed phase. Phys. Fluids **A3**, 2260–2275 (1991)
5. M. Born, H.S. Green, A kinetic theory of liquids. Nature **4034**, 251–254 (1947)
6. D.W. Brenner, Empirical potential for hydrocarbons for use in simulating the chemical vapor deposition of diamond films. Phys. Rev. B **42**, 9458–9471 (1990)
7. H.K. Cammenga, in *Current Topics in Materials Science,* vol. 5, ed. by E. Kaldis. (North-Holland, Amsterdam, 1980), pp. 335–446
8. C. Cercignani, *Rarefied Gas Dynamics* (Cambridge University Press, New York, NY, 2000)
9. S. Chapman, T.G. Cowling, *The Mathematical Theory of Non-uniform Gases,* 3rd edn. (Cambridge University Press, Cambridge, 1990)
10. J.H. Dymond, B.J. Alder, Pair potential for argon. J. Chem. Phys. **51**, 309–320 (1969)
11. J.M. Hale, *Molecular Dynamics Simulation, Elementary Methods* (Wiley, New York, NY, 1992)
12. C.D. Holcomb, P. Clancy, S.M. Thompson, J.A. Zollweg, A critical study of simulations of the Lennard-Jones liquid – vapor interface. Fluid Phase Equilib. **75**, 185–196 (1992)
13. W.G. Hoover, *Molecular Dynamics*. Lecture notes in physics vol. 258, (Springer, Berlin, 1986)
14. M. Inaba, S. Fujikawa, T. Yano, *Molecular gas dynamics on condensation and evaporation of water induced by sound waves*. *Rarefied Gas Dynamics.* AIP Conference Proceedings, vol. 1084 (AIP, Melville, NY, 2009), pp. 671–676
15. J.H. Irving, J.G. Kirkwood, The statistical mechanical theory of transport processes. IV. The equations of hydrodynamics. J. Chem. Phys. **18**, 817–829 (1950)
16. T. Ishiyama, T. Yano, S. Fujikawa, Molecular dynamics study of kinetic boundary condition at an interface between argon vapor and its condensed phase. Phys. Fluids **16**, 2899–2906 (2004)
17. T. Ishiyama, T. Yano, S. Fujikawa, Molecular dynamics study of kinetic boundary condition at an interface between a polyatomic vapor and its condensed phase. Phys. Fluids **16**, 4713–4726 (2004)
18. T. Ishiyama, T. Yano, S. Fujikawa, Kinetic boundary condition at a vapor – liquid interface. Phys. Rev. Lett. **95**, 084504 (2005)
19. W.L. Jorgensen, Optimized intermolecular potential functions for liquid alcohols. J. Phys. Chem. **90**, 1276–1284 (1986)
20. W.L. Jorgensen, J. Chandrasekhar, J.D. Madura, R.W. Impey, M.L. Klein, Comparison of simple potential functions for simulating liquid water. J. Phys. Chem. **79**, 926–935 (1983)
21. K. Kobayashi, S. Watanabe, D. Yamano, T. Yano, S. Fujikawa, Condensation coefficient of water in a weak condensation state. Fluid Dyn. Res. **40**, 585–596 (2008)
22. L.D. Landau, E.M. Lifshitz, *Statistical Physics,* 3rd edn. Part 1, Volume 5 of Course of Theoretical Physics (Elsevier, Amsterdam, 1980)
23. J.E. Lennard-Jones, The equation of state of gases and critical phenomena. Physica **4**, 941–956 (1937)
24. E.M. Lifshitz, L. Pitaevskii, *Physical Kinetics*. Volume 10 of Course of Theoretical Physics (Elsevier, Amsterdam, 1980)
25. M. Matsumoto, Molecular dynamics of fluid phase change. Fluid Phase Equilib. **144**, 307–314 (1998)
26. M. Mecke, J. Winkelmann, J. Fisher, Molecular dynamics simulation of the liquid-vapor interface: The Lennard-Jones fluid. J. Chem. Phys. **107**, 9264–9270 (1997)
27. G. Nagayama, T. Tsuruta, A general expression for the condensation coefficient based on transition state theory and molecular dynamics simulation. J. Chem. Phys. **118**, 1392–1399 (2003)
28. NIST Chemistry WebBook, http://webbook.nist.gov/chemistry/

29. W.H. Press, S.A. Teukolsky, W.T. Vetterling, B.P. Flannery, *Numerical Recipes,* 3rd edn. The Art of Scientific Computing (Cambridge University Press, Cambridge, 2007)
30. F. Reif, *Fundamentals of Statistical and Thermal Physics* (Waveland Press, Long Grove, IL, 2009)
31. P. Résiboirs, M. De Leener, *Classical Kinetic Theory of Fluids* (Wiley New York, NY, 1977)
32. A. Sommerfeld, *Thermodynamics and Statistical Mechanics*. Lectures on theoretical physics, vol V (Academic, New York, NY, 1964)
33. Y. Sone, Kinetic theory of evaporation and condensation – linear and nonlinear problems. J. Phys. Soc. Jpn. **45**, 315–320 (1978)
34. Y. Sone, *Kinetic Theory and Fluid Dynamics* (Birkhäuser, Boston, MA, 2002)
35. Y. Sone, *Molecular Gas Dynamics* (Birkhäuser, Boston, MA, 2007)
36. Y. Sone, Y. Onishi, Kinetic theory of evaporation and condensation – hydrodynamic equation and slip boundary condition. J. Phys. Soc. Jpn. **44**, 1981–1994 (1978)
37. Y. Sone, K. Aoki, T. Doi, Kinetic theory analysis of gas flows condensing on a plane condensed phase: Case of a mixture of a vapor and a noncondensable gas. Transp. Theory Stat. Phys. **21**, 297–328 (1992)
38. Y. Sone, K. Aoki, S. Takata, H. Sugimoto, A.V. Bobylev, Inappropriateness of the heat-conduction equation for description of a temperature field of a stationary gas in the continuum limit: Examination by asymptotic analysis and numerical computation of the Boltzmann equation. Phys. Fluids **8**, 628–638 (1996); Erratum, ibid. **8**, p. 841.
39. S. Takata, K. Aoki, Two-surface problems of a multicomponent mixture of vapors and noncondensable gases in the continuum limit in the light of kinetic theory. Phys. Fluids, **11**, 2743–2756 (1999)
40. A. Trokhymchuk, J. Alejandre, Computer simulations of liquid/vapor interface in Lennard-Jones fluids: Some questions and answers. J. Chem. Phys. **111**, 8510–8523 (1999)
41. T. Tsuruta, G. Nagayama, Molecular dynamics study on condensation coefficients of water. Trans. Jpn. Soc. Mech. Eng. **68**, 1898–1904 (2002) (in Japanese)
42. T. Yano, Half-space problem for gas flows with evaporation or condensation on a planar interface with a general boundary condition. Fluid Dyn. Res. **40**, 474–484 (2008)
43. T. Yano, K. Kobayashi, S. Fujikawa, *Condensation of methanol vapor onto its liquid film on a solid wall behind a reflected shock wave. Rarefied Gas Dynamics*. AIP Conference Proceedings, vol. 762 (AIP, Melville, NY, 2005), pp. 208–213

http://www.springer.com/978-3-642-18037-8

Vapor-Liquid Interfaces, Bubbles and Droplets
Fundamentals and Applications
Fujikawa, S.; Yano, T.; Watanabe, M.
2011, XIV, 230 p., Hardcover
ISBN: 978-3-642-18037-8